Methods[1]

Expedition 327 Scientists[2]

Chapter contents

[1] Expedition 327 Scientists, 2011. Methods. *In* Fisher, A.T., Tsuji, T., Petronotis, K., and the Expedition 327 Scientists, *Proc. IODP,* 327: Tokyo (Integrated Ocean Drilling Program Management International, Inc.). doi:10.2204/iodp.proc.327.102.2011
[2] Expedition 327 Scientists' addresses.

Introduction

This introductory section provides an overview of operations, depth conventions, curatorial procedures, and general core handling and analysis. This information will help the reader understand the basis of our shipboard observations and preliminary interpretations. It will also enable interested investigators to identify data and select samples for further analysis. The information presented here concerns mainly shipboard operations and analyses described in the site chapters, including a small number of shipboard samples that were analyzed on shore because of a lack of time or necessary instrumentation during Integrated Ocean Drilling Program (IODP) Expedition 327. Methods used by various investigators for shore-based analyses of Expedition 327 samples and data associated with separate scientific studies will be described in individual publications in professional journals.

Site locations

GPS coordinates from precruise site surveys or preexisting Ocean Drilling Program (ODP) and IODP sites were used to position the R/V *JOIDES Resolution* at Expedition 327 sites. A SyQwest Bathy 2010 CHIRP subbottom profiler was used to monitor seafloor depth on the approach to each site to confirm depth profiles from precruise surveys or previous expeditions. Once the vessel was positioned at a site, the thrusters were lowered and a positioning beacon was dropped to the seafloor. The dynamic positioning (DP) control of the vessel uses navigational input from the GPS system and triangulation to the seafloor beacon, weighted by the estimated positional accuracy. The final hole position was the mean position calculated from the GPS data collected over a significant portion of the time the hole was occupied.

Drilling operations

The advanced piston corer (APC), extended core barrel (XCB), and rotary core barrel (RCB) systems were used during Expedition 327.

The APC and XCB systems were used to recover the sedimentary section and sediment/basalt interface at Site U1363. The RCB system was used to recover the basement section at Site U1362.

The APC system cuts soft-sediment cores with minimal coring disturbance relative to other IODP coring systems. After the APC core barrel is lowered through the drill pipe and lands near the

doi:10.2204/iodp.proc.327.102.2011

bit, the drill pipe is pressured up until the two shear pins that hold the inner barrel attached to the outer barrel fail. The inner barrel then advances into the formation and cuts the core. The driller can detect a successful cut, or "full stroke," from observation of the pressure gauge on the rig floor because the excess pressure accumulated prior to the stroke drops rapidly.

APC refusal is conventionally defined in two ways: (1) the piston fails to achieve a complete stroke (as determined from the pump pressure reading) because the formation is too hard or (2) excessive force (>60,000 lb; ~267 kN) is required to pull the core barrel out of the formation. When a full or partial stroke can be achieved but excessive force cannot retrieve the barrel, the core barrel can be "drilled over" (i.e., after the inner core barrel is successfully shot into the formation, the drill bit is advanced to total depth to free the APC barrel).

The XCB system was used to advance the hole when APC refusal occurred before the target depth was reached or when drilling conditions required it. The XCB is a rotary system with a small cutting shoe that extends below the large rotary APC/XCB bit. The smaller bit can cut a semi-indurated core with less torque and fluid circulation than the main bit, potentially improving recovery. The XCB cutting shoe (bit) extends ~30.5 cm ahead of the main bit in soft sediments but retracts into the main bit when hard formations are encountered.

The bottom-hole assembly (BHA) used for APC and XCB coring was composed of an 11$^{7}/_{16}$ inch (~29.05 cm) drill bit, a bit sub, a seal bore drill collar, a landing saver sub, a modified top sub, a modified head sub, five 8¼ inch control length drill collars, a tapered drill collar, two stands of 5½ inch transition drill pipe, and a crossover sub to the drill pipe that extended to the surface.

The RCB BHA included a 9⅞ inch RCB drill bit, a bit sub, an outer core barrel, a modified top sub, a modified head sub, a variable number of 8¼ inch control length drill collars, a tapered drill collar, and two stands of 5½ inch drill pipe. The number of drill collars ranged from 8 to 26 during coring so that it was possible to position only 8¼ inch collars (rather than drill pipe) in the open hole. Keeping drill collars in the open hole helped to prevent basement rubble from falling in the hole, which could have caused the drill pipe to become stuck. Drill collars also help to maintain annular velocities that lift cuttings from the hole during drilling.

We did not use nonmagnetic core barrels because of the nature of the formation and did not orient cores because of the lack of high-priority scientific goals requiring this procedure. Formation temperature measurements were made at Site U1363 to determine heat flow through the sedimentary section (see **"Downhole measurements"**).

Most APC/XCB cored intervals were ~9.5 m long, which is the length of a standard core barrel and the length of a joint of drill pipe. In some cases the drill string was drilled or "washed" ahead without recovery to advance the drill bit to the target depth at which core recovery needed to resume. Depths of drilled intervals and core recovery are provided in the "Operations" section of each site chapter.

IODP depth conventions

Deep Sea Drilling Project (DSDP), ODP, and IODP Phase 1 reports, diagrams, and publications used three primary designations to reference depth: meters below rig floor (mbrf), meters below seafloor (mbsf), and meters composite depth (mcd). These designations were combinations of origin of depth (rig floor or seafloor), measurement units (meters), and method of construction (composite). The designations evolved over many years to meet the needs of individual science parties.

Over the course of ODP and IODP scientific drilling, issues with the existing depth scale designations and the lack of a consistent framework became apparent. For example, the application of the same designation to scales created with distinctly different tools and methods was common (e.g., mbsf being used for scales measured both by drill string tally and the wireline). Consequently, new scale type designations were created ad hoc to differentiate the wireline logging scale from the core depth scale so that depth-mapping procedures and products could be adequately described. However, the management and use of depth scales and splices for a site was problematic, and the requirement to integrate scientific procedures among three IODP implementing organizations (IOs) amplified the need to establish a standardized and versatile depth framework.

A new classification and nomenclature for depth scale types was defined in 2006–07 during the hiatus in IODP drilling operations to provide a starting point from which the IOs could address more specific issues about the management of depth scales and splices (see "IODP Depth Scales Terminology" at **www.iodp.org/program-policies/**) (Table **T1**). This new depth framework has been implemented in the Laboratory Information Management System (LIMS) used aboard the *JOIDES Resolution*.

The new methods and nomenclature used to calculate sample depth in a hole are now method specific, which ensures that data acquisition, scale mapping,

and construction of composite splices are unequivocal.

The primary depth scales are measured by the length of drill string (e.g., drilling depth below rig floor [DRF] and drilling depth below seafloor [DSF]), length of core recovered (e.g., core depth below seafloor [CSF] and core composite depth below seafloor [CCSF]), and logging wireline (e.g., wireline log depth below rig floor [WRF] and wireline log depth below seafloor [WSF]). In cases where multiple logging passes are made, logs are mapped to one reference pass, creating the wireline log matched depth below seafloor (WMSF). All units are in meters. The relationship between scales is defined by protocol, such as the rules for computation of CSF from DSF, or user-defined correlations, such as core-to-log correlation or stratigraphic correlation of cores between holes to create a common CCSF scale from the CSF scale used in each hole. The distinction in nomenclature should keep the reader aware that a nominal depth value at different depth scales usually does not refer to the exact same stratigraphic interval.

During Expedition 327, unless otherwise noted, depths below rig floor were calculated as DRF and are reported as meters; core depths below seafloor were calculated as CSF Method A (CSF-A) and are reported as mbsf; and all downhole wireline depths were calculated as WMSF and are reported as mbsf (Table T1). In addition, some depths are reported in meters subbasement (msb), accounting for the thickness of the sediment section above the volcanic crust, because this depth reference is relevant to numerous aspects of borehole observatory system design and installation and to cross-hole lithologic correlation.

Core handling and analysis

Cores were extracted from the core barrel in plastic liners. The liners were carried from the rig floor to the core processing area on the catwalk outside the core laboratory, where they were split into ~1.5 m sections. Blue (uphole direction) or clear (downhole direction) liner caps were glued with acetone onto the cut liner sections.

Hard rocks

Pieces were pushed to the bottom of 1.5 m liner sections, and the total rock length was measured. The length was entered into the database as "created length" using the SampleMaster application. This number was used to calculate recovery. The liner sections were transferred to the core splitting room.

Whole-round samples were taken for microbiological analyses following consultation with other members of the science party. The imaging specialist took photographs of these samples before they were bagged and processed. In cases where a whole round was removed, a yellow cap was used to denote the missing interval.

The plastic liners were split lengthwise to expose the core. Oriented pieces of core were marked on the bottom with a red wax pencil to preserve orientation. In some cases pieces were too small to be oriented with certainty. Adjacent but broken pieces that could be fit together along fractures were curated as single pieces. The petrologist or assistant laboratory officer on shift confirmed piece matches and marked the split line on the pieces, which defined how the pieces were to be cut into two equal halves. The aim was to maximize the expression of dipping structures on the cut face of the core while maintaining representative features in both archive and working halves. A plastic spacer was secured with acetone to the split core liner between individual pieces or reconstructed contiguous groups of subpieces. These spacers may represent substantial intervals of no recovery. The length of each section of core, including spacers, was entered into the database as "curated length," which commonly differs by a few to several centimeters from the length measured on the catwalk. The depth of each piece was recalculated in the database on the basis of its curated length.

Core sections were placed in core racks in the laboratory. When the cores reached equilibrium with laboratory temperature (typically after 3–4 h), the whole-round core sections were run through the Natural Gamma Radiation Logger (NGRL) and the Whole-Round Multisensor Logger (WRMSL), which was configured for hard rock to measure magnetic susceptibility and gamma ray attenuation.

Each piece of core was split with a diamond-impregnated saw into an archive half and a working half, with the positions of plastic spacers between pieces maintained in both halves. Pieces were numbered sequentially from the top of each section, beginning with 1. Separate subpieces within a single piece were assigned the same number but were lettered consecutively (e.g., 1A, 1B, 1C, etc.). Pieces were labeled only on the outer cylindrical surfaces of the core. An arrow pointing to the top of the section was added to the label of each oriented piece, and the orientation was recorded in the database using the SampleMaster application.

The working half of each core was sampled for shipboard physical properties, bulk X-ray diffraction (XRD) and inductively coupled plasma–atomic emission spectroscopy (ICP-AES) analyses, and thin sections. Thermal conductivity measurements were taken on selected samples (see **"Physical properties"**).

The archive half of each core was scanned on the Section Half Imaging Logger (SHIL) and measured for color reflectance and point magnetic susceptibility on the Section Half Multisensor Logger (SHMSL). The archive halves were also described visually and by means of thin sections. Some archive-half sections or pieces were run through the cryogenic magnetometer.

Sampling for shore-based studies was delayed until the end of coring in each hole, except when samples had to be taken rapidly, generally for microbiology studies. Sampling was conducted based on the sampling plan agreed upon by the science party and shipboard curator.

Sediments

Once the cores were cut into sections, whole-round samples were taken for microbiological or pore water analyses. When a whole round was removed, a yellow cap was used to denote the missing interval.

Core sections were placed in core racks in the laboratory. When the cores reached equilibrium with laboratory temperature (typically after 3–4 h), whole-round core sections were run through the WRMSL to measure *P*-wave velocity, resistivity, magnetic susceptibility, and bulk density. Thermal conductivity measurements were taken at varying intervals (see **"Physical properties"**).

Sediment cores were split lengthwise from bottom to top into working and archive halves. Investigators should note that older material may have been transported upward on the split face of each section during splitting. The working half of each core was sampled for various shipboard analyses. The working half of each core was also sampled for shore-based studies based on the sampling plan agreed upon by the science party and shipboard curator.

The archive half of each core was scanned on the SHIL and measured for color reflectance and magnetic susceptibility on the SHMSL. At the same time, the archive halves were described visually and by means of smear slides. Finally, some of the archive halves were run through the cryogenic magnetometer.

For both sediments and hard rocks, cores were put into labeled plastic bags, sealed, and transferred to cold storage space aboard the ship. At the end of the expedition the cores were transferred from the ship into refrigerated trucks and transported to cold storage at the IODP Gulf Coast Repository in College Station, Texas (USA).

Curatorial procedures and sample depth calculations

Numbering of sites, holes, cores, and samples follows standard IODP procedure. A full curatorial identifier for a sample consists of the following information: expedition, site, hole, core number, core type, section number, archive or working half (if taken from a section half), piece number (hard rocks only), and interval in centimeters, as measured from the top of the core section. For example, a sample identification of "327-U1362A-5R-2 (Piece 1, 4–7 cm)" indicates a 3 cm sample of Piece 1 removed from the interval between 4 and 7 cm below the top of Section 2 of Core 5 of Hole A at Site U1362 during Expedition 327 (Fig. **F1**). The "U" preceding the hole number indicates the hole was drilled by the US implementing organization (USIO) platform, the *JOIDES Resolution*. The drilling system used to obtain a core is designated in the sample identifiers as follows:

R = RCB.
H = APC.
X = XCB.

Core intervals are defined by the length of drill string, the seafloor depth, and the amount the driller advanced the core barrel; they are reported in DSF. The length of the core is defined by the sum of the lengths of the core sections. The CSF depth of a sample is calculated by adding the offset of the sample below the section top and the lengths of all higher sections in the core to the core-top depth measured with the drill string (DSF). A soft to semisoft sediment core from less than a few hundred meters below seafloor expands upon recovery (typically a few percent to as much as 15%), so the recovered interval does not match the cored interval. In addition, a coring gap typically occurs between cores, as shown by composite depth construction. Thus, a discrepancy between DSF and CSF depths can exist with regard to a stratigraphic interval. Furthermore, when core recovery is >100% of the cored interval, a sample taken from the bottom of a core will have a CSF depth deeper than that of a sample from the top of the subsequent core (i.e., the data associated with the two core intervals overlap).

If a core has incomplete recovery, for curation purposes all cored material is assumed to originate from the top of the drilled interval as a continuous section; the true depth interval within the cored interval is unknown. This should be considered a sampling uncertainty in age-depth analysis or correlation of core data with downhole logging data.

Core sample disturbance

Cores may be significantly disturbed and contain extraneous material as a result of the coring and core handling process. In formations with loose sand layers, sand from intervals higher in the hole may be washed down by drilling circulation, accumulate at the bottom of the hole, and be sampled with the next core. The uppermost 10–50 cm of each core must therefore be examined critically during description for potential "fall-in." Common coring-induced deformation includes the concave-downward appearance of originally horizontal bedding. Piston action may result in fluidization ("flow-in") at the bottom of APC cores. Retrieval from depth to the surface may result in elastic rebound. Gas that is in solution at depth may become free and drive core segments within the liner apart. When gas content is high, pressure must be relieved for safety reasons before the cores are cut into segments. This is accomplished by drilling holes into the liner, which forces some sediment as well as gas out of the liner. These disturbances are described in each site chapter and graphically indicated on the visual core descriptions (VCDs), also known as "barrel sheets."

Petrology, hard rock geochemistry, and structural geology

Core curation and shipboard sampling

Core handling protocols are described in **"Core handling and analysis"** in the "Introduction." To preserve important features and structures, core sections containing igneous rocks were examined before the core was split, allowing orientation of individual pieces. To minimize contamination of the core with platinum group elements and gold, the describers removed jewelry from their hands and wrists before handling the core. The archive half of each core was described using the DESClogik core description program, and a summary VCD was produced for each section.

Lithologic units and subunits were identified on the basis of the presence of contacts, chilled margins, changes in primary mineralogy (occurrence and abundance), color, grain size, and structural or textural variations. Unit boundaries were generally chosen to indicate different volcanic cooling units, although limited recovery in some cases resulted in arbitrary placement of a unit boundary between samples having different lithologies. In order to preserve important information about volcanology without defining an unreasonable number of units within a single core, subunits were designated when there were frequent changes in texture without accompanying changes in mineralogy (for example, several pieces containing glass within 50 cm of core, all of which are mineralogically similar).

Hard rock visual core descriptions

Hard rock VCD (HRVCD) forms were generated for each section of basement core recovered. A key to the symbols used on the HRVCDs is provided in Figure **F2.** Each HRVCD form contains the following information (from left to right):

1. Depth
2. Core length scale
3. Piece number
4. Core image
5. Orientation
6. Shipboard samples
7. Lithologic unit
8. Veins
9. Structures
10. Structure measurement
11. Glass
12. Phenocrysts
13. Groundmass grain size
14. Alteration

Upward arrows on the HRVCD forms indicate vertically orientated pieces of core. The location and purpose of samples taken for shipboard analyses are marked with the appropriate notation (Fig. **F2**). The lithologic unit column records the position of unit and subunit boundaries by solid (unit) and dashed (subunit) horizontal lines. Lithologic units are numbered and increase downhole; unit numbers followed by capital letters denote subunits. The structural column has symbols to represent the location and type of observed structural features. Structural measurements (indicated by boxes) can be obtained from the database. In addition to the graphical logs, a short unit summary is provided on the right-hand side of the HRVCD. This summary contains the following information:

1. Expedition, hole, core, and section numbers
2. Unit number
3. Rock name
4. Summary description
5. Pieces
6. Contacts
7. Color
8. Phenocrysts
9. Groundmass
10. Glass

11. Vesicles
12. Alteration
13. Veins
14. Structure
15. Physical properties

Igneous petrology

Each unit and subunit was described in terms of groundmass, primary mineralogy, color, vesicles, and igneous contacts. Each of these observations was recorded using the DESClogik program and uploaded to the LIMS database.

Units and subunits were defined on the basis of groundmass texture and abundance of primary minerals. Basalts were defined in hand specimens by the identification and abundance of phenocrysts:

Aphyric = <1% phenocrysts.
Sparsely phyric = 1%–5% phenocrysts.
Moderately phyric = >5%–10% phenocrysts.
Highly phyric = >10% phenocrysts.

Igneous units were further classified by the type of phenocryst present. For naming purposes, phenocrysts are listed in order of lowest to highest abundance (e.g., "plagioclase-olivine phyric" indicates that olivine abundance is greater than plagioclase abundance).

Rock color was determined on a wet cut surface of the core using the Munsell color chart. Groundmass character was assessed using a binocular microscope and defined by average grain size (the width of elongated grains) and classified as follows:

G = glassy.
cx = cryptocrystalline (<0.1 mm).
µx = microcrystalline (0.1–0.2 mm).
fg = fine grained (>0.2–1 mm).
mg = medium grained (>1 mm).

The abundance of vesicles was estimated and ranked using the following scale:

Nonvesicular = <1%.
Sparsely vesicular = 1%–5%.
Moderately vesicular = >5%–20%.
Highly vesicular = >20%.

The size and shape (sphericity and roundness) of vesicles were also recorded. Description of vesicle-filling phases can be found in **"Alteration."** For graphical simplicity, documentation of vesicles in the graphical logs of the HRVCDs was limited to occurrences of high vesicularity.

Breccia samples were described by clast and matrix. Clast abundance, size, shape, sorting, composition, and alteration were noted. Matrix was described in terms of volume, composition, structure, and alteration, and cement was described in terms of volume and composition. Each breccia was classified as hydrothermal, magmatic, or tectonic in origin:

Bm = magmatic (breccias containing glass or quench textures, such as hyaloclastites, and pillow breccias and primary matrix minerals).
Bh = hydrothermal (breccias with secondary matrix or vein minerals).
Bc = tectonic (cataclasites and fault-gouges in which the matrix consists of the same material as the host rock).

Classification of igneous units as pillow basalt, basalt flows, and sheet flows was based on the nature of the recovered contacts and margins. Pillow basalts were characterized by curved margins (oblique to the vertical axis of the core) or by the presence of variolitic texture, curved fractures, or micro- to cryptocrystalline groundmass grain size. Basalt flows were assigned to units with chilled margins that lacked definitive pillow structure (curved margins). Sheet flows were identified by planar subhorizontal chilled margins and an increase in grain size in the center of the unit. Other rock types identified were breccias (magmatic and tectonic).

Alteration

Virtually all igneous rocks recovered during Expedition 327 have undergone alteration. This alteration manifests in four general forms: (1) replacement of groundmass, (2) replacement of phenocrysts, (3) hydrothermal veins and alteration halos, and (4) lining and filling vesicles. Each of these alteration types was described and recorded separately and combined into a brief summary on the HRVCD forms. In addition, an alteration log recording the background alteration color and halo color for each individual piece is available in ALTLOG in **"Supplementary material."**

Background alteration type was defined by rock color and calibrated by thin section observations. Alteration intensity was assigned using the following scale:

Fresh = <2% alteration.
Slight = 2%–10% alteration.
Moderate = >10%–50% alteration.
High = >50%–90% alteration.
Complete = >90%–100% alteration.

The abundance of volcanic glass, both total and fresh percents, was recorded. The abundance and composition of infilling by secondary minerals was described for vesicles. Where possible, the successive infilling of vesicles was used to deduce the order of precipitation of secondary phases. Halos surrounding infilled vesicles were described by size, color, and

most abundant secondary mineral, where distinguishable.

A detailed vein log recording the presence, location, width, crosscutting relationships, shape, composition percent, color, and width of associated halos of each vein was made (see Site U1362 vein log in "Core descriptions" and VEINLOG in "Supplementary material"). Structural measurements undertaken on the veins were recorded and are described in "Structural geology."

Thin sections

Thin sections of basement rocks were studied to complete and refine igneous and alteration hand specimen observations. At least one representative thin section was produced for each unit. All thin section observations were recorded in the DESClogik program and entered into the LIMS database. These observations included textural features that were not identified in hand specimens; precise determination of the grain size of phenocrysts and groundmass; mineralogy, abundance, and type of glomerocrysts; presence of inclusions within phenocrysts; and presence of minor phases such as spinel, oxides, and sulfides. Crystal sizes (minimum, maximum, and average) of all primary phases were measured, and mineral morphologies and textural features were recorded. When replacement of primary phases by secondary phases was observed, abundance, composition, and textural occurrence were recorded.

The terms "heterogranular" (different crystal sizes), "seriate" (continuous range in grain size), "porphyritic" (indicating the presence of phenocrysts), or "glomeroporphyritic" (containing clusters of phenocrysts) were applied to groundmass texture. Groundmass was also classified as hypocrystalline (100% crystals) to hypohyaline (100% glass), variolitic, intergranular (olivine and pyroxene grains between plagioclase laths), intersertal, subophitic, or ophitic. The same terminology was used for thin section and macroscopic descriptions.

An example of the thin section description form is given in Figure F3. Thin section descriptions are included in this volume (see "Core descriptions") and available from the IODP database. Digital photomicrographs were taken during the cruise to document features described in the thin sections. Selected images are available in the "Site U1362" chapter and in PHOTOMIC in "Supplementary material."

Modal estimation of phenocryst phases in thin section was made using scanned images of the whole thin section and Adobe Photoshop software. This method is described in detail in the Expedition 309/312 *Proceedings* volume (Expedition 309/312 Scientists, 2006) and is briefly summarized here. This method is less labor intensive and more accurate for estimating phenocryst abundances. As with any method based on a single thin section, the applicability of the method to larger volumes depends on an assumption of homogeneity that may or may not be valid.

For each thin section, a full-page scanned image was made, and phenocryst phases were marked on an acetate overlay. The acetate overlays were scanned and saved as native Adobe Photoshop files. The threshold function was used to separate the phenocrysts, marked by black, from the background. The histogram function of Photoshop was then used to determine the total number of pixels and the number of pixels represented by the phenocryst phase. Using this ratio the modal percentage of the phenocryst phase was calculated. This method can also be used for multiple phenocryst phases by erasing and subtracting the pixels associated with each phase.

Structural geology

This section outlines the techniques used for the description of structural features observed in hard rock basement cores. Conventions for structural studies adopted during previous ODP hard rock drilling legs (Shipboard Scientific Party, 1989, 1991, 1992a, 1992c, 1992d, 1993a, 1993b, 1995, 1999, 2003) were generally followed during Expedition 327.

Graphical representation and terminology

All material from both working and archive halves was examined, although all structure and orientation measurements were made on the archive halves. The most representative structural features in the cores are summarized on the HRVCD forms (see "Core descriptions"). All structural data were entered into the DESClogik program.

To maintain consistency in core descriptions we used a set of structural feature identifiers. Brittle deformation identifiers include "joint," "vein," "shear vein," "fault," and "breccia." Identification of these features was based on the presence of fractures, filling phases, and evidence of shear displacement. The terminology adopted generally follows that of Ramsay and Huber (1987), Twiss and Moores (1992), and Passchier and Trouw (1996) and is consistent with the terminology used during previous ODP/IODP legs and expeditions (e.g., ODP Leg 153 terminology was used for brittle deformation [Shipboard Scien-

tific Party, 1995]). Some of the terms commonly used in the structural descriptions are illustrated in Figure F4 (Expedition 301 Scientists, 2005a):

- J = joints (fractures where the two sides show no differential displacement relative to the naked eye or 10× hand lens and have no filling materials).
- V = veins (extensional open fractures filled with secondary minerals).
- SV = shear veins (obliquely opening veins with minor shear displacement filled with slicken-fibers or overlapping fibers).
- F = faults (fractures with kinematic evidence for shear displacement across the discontinuity or with an associated cataclasite; we adopted the term "microfault" when the scale of the offset was millimetric).

This division of structures does not imply that all features fall into distinct and exclusive categories. We prefer to use the term "veins" for all healed fractures, avoiding the usual division based on fracture width (e.g., Ramsay and Huber [1987] defined veins as having >1 mm filling material). Rigid boundaries between the adopted structural categories do not exist. Where necessary, details specific to structural features are illustrated with comments and sketches.

Geometric reference frame

Structures were measured on archive halves relative to the core reference frame used by IODP. The plane normal to the axis of the borehole was referred to as the horizontal plane. On this plane, a 360° net was used with a pseudosouth (180°) pointing into the archive half and a pseudonorth (0°) pointing out of the archive half and perpendicular to the cut surface of the core. The cut surface of the core, also called "core face" or "cut face," therefore is a vertical plane striking 90°–270°. The strike of planar features across the cut face of the archive half was measured with 0° down the vertical axis of the core, and the dip was measured using the right-hand rule (Fig. F5). The measured orientations were rotated into the IODP reference frame using stereonet software.

Hard rock geochemistry

Shipboard analyses

Sample preparation

Representative samples of igneous rocks were analyzed for major and trace elements during Expedition 327 using ICP-AES. Samples of ~10 cm^3 were cut from the core with a diamond saw blade. All outer surfaces were ground on a diamond-impregnated disk to remove altered rinds and contamination resulting from cutting and drilling processes. Cleaned samples were then placed individually into beakers containing trace metal-grade methanol and were washed ultrasonically for 15 min. The methanol was decanted, and the samples were washed twice in an 18 MΩ deionized water ultrasonic bath for 10 min. The clean pieces were dried for 10–12 h at 110°C.

The clean, dry whole-rock samples were crushed to <1 cm chips between two disks of Delrin plastic in a hydraulic press. The chips were ground to a fine powder in a tungsten carbide SPEX 8000M mixer/mill or, for larger samples, a SPEX 8515 shatterbox. A 1.0 ± 0.0005 g aliquot of the sample powder was weighed on a Mettler Toledo dual balance system and ignited to determine weight loss on ignition (LOI).

ODP *Technical Note* 29 (Murray et al., 2000) describes in detail the shipboard procedure for digestion of rocks and ICP-AES analysis of samples. The following protocol is an abbreviated form of this procedure, with minor modifications. After determination of LOI, 100.0 ± 0.2 mg aliquots of the ignited whole-rock powders were weighed and mixed with 400.0 ± 0.5 mg of $LiBO_2$ flux that had been preweighed on shore. Standard rock powders and full procedural blanks were included with unknowns in each ICP-AES run. All samples and standards were weighed ±0.2 mg on the Cahn C-31 microbalance (designed for onboard measurements), with weighing errors estimated to be ±0.05 mg under relatively smooth sea-surface conditions.

Next, 10 mL of 0.172 mM aqueous LiBr solution was added to the mixture of flux and rock powder as an antiwetting agent to prevent the cooled bead from sticking to the crucible. Samples were then fused individually in Pt-Au (95:5) crucibles for 12 min at a maximum temperature of 1050°C in a Bead Sampler NT-2100. After cooling, beads were transferred to 125 mL high-density polyethylene (HDPE) bottles and dissolved in 50 mL of 10% HNO_3. Following digestion of the bead, all of the solution was passed through a 0.45 µm filter into a clean 60 mL wide-mouth HDPE bottle. Next, 2.5 mL of this solution was transferred to a plastic vial and diluted with 17.5 mL of 10% HNO_3 to bring the total volume to 20 mL. The final solution-to-sample dilution factor was ~4000.

Analyses

Major (Si, Ti, Al, Fe, Mn, Mg, Ca, Na, K, and P) and trace (Ba, Sr, Zr, Y, V, Sc, Cu, Zn, Co, Cr, and Ni) element concentrations of standards and samples were determined with a Teledyne Leeman Labs Prodigy ICP-AES instrument. Specific analytical conditions for each sample run are provided in Table T2. For

several elements, measurements were made at two wavelengths (e.g., Si was measured at 251.611 and 288.158 nm). In such cases, the reported values were obtained by averaging the data.

The plasma was ignited at least 30 min before each sample run to allow the instrument to warm up and stabilize. A peak profile alignment was then performed using basalt laboratory standards BHVO-2 (US Geological Survey) or BIR-1 (Govindaraju, 1989) in 10% HNO_3. During the initial setup, an emission profile was selected for each peak to determine peak-to-background intensities and to set the locations of background levels for each element. The Prodigy software uses these background locations to calculate the net intensity for each emission line. The photomultiplier voltage was optimized by automatically adjusting the gain for each element using BHVO-2.

ICP-AES data presented in "Geochemistry" in the "Site U1362" chapter were attained by integrating the area under the curves for wavelength versus response plots. Each sample was analyzed three times from the same dilute solution within a given sample run. For elements measured at two wavelengths we either used the wavelength giving the better calibration line in a given run or, if the calibration lines for both wavelengths were of similar quality, used the data for both and reported the average concentration.

A typical ICP-AES run (Table T2) included

- A set of eight certified rock standards (BCR-2, BIR-1, JA-3, JGb-1, JR-2, NBS-1c, SCO-1, and STM-1) analyzed at the beginning of each run and again after every 20 samples;
- As many as 15 unknown samples analyzed in triplicate;
- A drift-correcting standard (BHVO-2) analyzed in every fifth sample position and at the beginning and end of each run;
- Blank solutions analyzed near the beginning and end of each run and, in the longer runs, at another point in the middle of the sequence;
- Two "check" standards (BAS 206 and BAS 140) run as unknowns, each analyzed in triplicate at least twice during a run; and
- A 10% HNO_3 wash solution run for 60 s between each analysis.

Data reduction

Following each sample run the measured raw intensity values were transferred to a data file, corrected for instrument drift, and then corrected for the full procedural blank. Drift correction was applied to each element by linear interpolation between the drift-monitoring solutions run every fifth analysis. Following drift correction and blank subtraction, a calibration line for each element was calculated using the results for the certified rock standards. Element concentrations in the samples were then calculated from the relevant calibration lines.

Estimates of accuracy and precision for major and trace element analyses were based on replicate analyses of international standards (BCR-2), the results of which are presented in Table T3. In general, run-to-run relative precision by ICP-AES was <3% for the major elements. Run-to-run relative precision for trace elements was <10%. Exceptions typically occurred when the element in question was near background values.

Shore-based analyses

Epidote samples recovered from the drill bit in Hole U1362A were analyzed using a tabletop Hitachi TM1000 scanning electron microscope (SEM) at the National Oceanography Centre, University of Southampton, UK, following methods described by Hunt et al. (2010). This SEM energy dispersive spectrometry methodology enables nonpretreated samples to be analyzed, akin to the EAGLE III µXRF.

Lithostratigraphy

Note: This section was contributed by Sarah-Jane Jackett (Integrated Ocean Drilling Program, Texas A&M University, 1000 Discovery Drive, College Station TX 77845, USA).

The lithostratigraphic procedures used during Expedition 327, including sediment classification, visual core description, smear slide preparation and description, and XRD, are outlined below.

Core preparation

Prior to description, the quality of the split surface of the archive half of each core was assessed and, where necessary (e.g., surface was smeared or uneven), scraped lightly with a glass slide. This improved the visibility of sedimentary structures and fabric.

Visual core description

Sediment components and percentages in the core were determined using a hand lens, binocular microscope, and smear slide examination. Information from macroscopic and microscopic examinations of each core section was entered into the DESClogik program. Before core description, a customized template was created for recording lithology, drilling disturbance, and bioturbation. A second template containing columns for texture and relative abundance

of biogenic/mineralogic components was configured specifically for recording smear slide data. DESClogik includes a graphic display mode for core data (e.g., digital images of section halves and measurement data) that can be used to augment core description. The data entered in DESClogik were uploaded into the LIMS database. The schemes used for sediment description are detailed below.

Lithologic classification

The lithologic classification scheme used during Expedition 327, modified after Shipboard Scientific Party (2004), is based on three end-member grain components: biogenic silica, carbonate, and terrigenous or volcanic grains, along with alternative modifiers determined from smear slides. This scheme is further divided according to the grain size of the terrigenous component (i.e., the relative proportions of sand, silt, and clay) (Wentworth, 1922) (Fig. F6). Adjectives such as "silty" and "clayey" are used to differentiate mixtures. Mixtures are divided on the basis of whether the silt content is greater than or less than 50% (silty clay mud or clayey silt, respectively). Sand is divided into fine sand and medium sand for description purposes.

Mixtures of terrigenous, siliceous, and calcareous sediments are named according to the relative proportion of the three components (Fig. F6). Sediment names also indicate the degree of sediment induration (e.g., clay versus claystone).

Color

Sediment color was determined qualitatively for core intervals using Munsell soil color charts (Munsell Color Company, Inc., 2000).

Sedimentary structures and lithologic accessories

Sedimentary structures, accessories, and other primary and secondary (diagenetic) features are noted in the core descriptions. Laminae are described as <1 cm thick. For turbidite sequences in which three lithologies are closely interbedded (i.e., the individual beds are <12 cm thick and alternate between the three lithologies), two interbedded lithology names are used (Fig. F6): interbedded fine sand-silt-clay and interbedded medium sand-silt-clay. When beds are scattered throughout a different lithology (e.g., beds of silt several centimeters to tens of centimeters thick within a clay bed), they are logged individually, and their associated thicknesses and textures are entered into the database using the DESClogik application.

Lithologic accessories noted include the presence of foraminifers, fossilized wood, glass, and mottles. Bioturbation is noted as either moderate or strong (Fig. F7).

Coring disturbance

The type and degree of coring disturbance are indicated according to the terminology defined in Figure F7.

Smear slide analysis

Toothpick samples were taken at select intervals in the core and used to create smear slides according to the method outlined in Mazzullo et al. (1988). One or more smear slide samples were collected from the main or dominant (D) lithology from the archive half of each core. Additional samples were collected from minor (M) lithologies or other areas of interest (e.g., laminations, mottles, etc.). Smear slides were viewed with a transmitted-light petrographic microscope, and the percentages of different mineralogic, biogenic, and authigenic components were estimated along with the proportions of sand, silt, and clay (terrigenous only). These estimations were recorded on smear slide sample sheets and entered into the database. This technique is limited in that sand grains are underemphasized, as are large calcareous components (shells and shell fragments), and the determination of percentages is subjective and varies slightly among different practitioners. Lithology descriptions from smear slides were calibrated by comparison with XRD analysis.

Standard graphic report (barrel sheet)

The LIMS2Excel application was used to extract data in a format that could be used to plot descriptive as well as instrument data in core graphic summaries using a commercial program (Strater, Golden Software). The Strater program was used to produce a simplified annotated standard graphic report, also known as a barrel sheet, for each core.

Beginning with the leftmost column, the barrel sheets display depth scale (CSF-A), core length, and section information. A fourth column displays the concatenated section-half images adjacent to a graphic lithology column in which core lithologies are represented by the graphic patterns illustrated in Figure F7. Subsequent columns provide information on drilling disturbance, sedimentary structures, lithologic accessories, and shipboard samples (Fig. F7). Additional columns present magnetic susceptibility (see **"Physical properties"**), color reflectance measurements, and Munsell color values.

X-ray diffraction analysis

Samples for XRD analyses were selected from working halves based on visual core observations (e.g., color variability, visual changes in lithology, and texture) and smear slides. XRD analyses were performed on three samples. Each 5–10 cm^3 sample was frozen, freeze-dried in the case of unlithified samples, and ground by hand or in an agate ball mill, as necessary. Prepared samples were top-mounted onto a sample holder and analyzed using a Bruker D-4 Endeavor diffractometer mounted with a Vantec-1 detector using nickel-filtered CuKα radiation. The standard locked coupled scan was as follows:

Voltage = 40 kV.
Current = 40 mA.
Goniometer scan = 5°–70°2θ.
Step size = 0.015°2θ.
Scan speed = 0.1 s/step.
Divergence slit = 0.3 mm.

Diffractograms of single samples were evaluated with the Bruker DiffracPlus software package, which allowed only for mineral identification and basic peak characterization (e.g., width and maximum peak intensity). Shipboard results yielded only qualitative results on the relative occurrences and abundances of the most common mineralogical components.

Pore water geochemistry

Shipboard interstitial water samples were obtained from 10–40 cm long whole-round samples cut on the catwalk. The samples were then capped and taken to the laboratory for immediate processing. Sampling resolution was 1–2 per core in the middle of the sediment column and ~1 per section (1.5 m) in the bottom 5 m of the sediment column. When there were too many interstitial water samples to process immediately, the capped whole-round samples were stored temporarily in the refrigerator at 4°C. Sediment processing for interstitial water sampling in the laboratory was carried out in a nitrogen-flushed and pressurized glove bag. After extrusion from the core liner, the outer layer of each whole-round sample was carefully scraped with a spatula to remove potential contamination from drill water (surface seawater). The remaining sediment was placed in a titanium squeezer modified after the standard stainless steel squeezer of Manheim and Sayles (1974). The piston was positioned on top of the squeezer, and the entire unit was removed from the glove bag and placed on the hydraulic press. Pressures as high as 76 MPa were applied in the squeezer, calculated from the measured hydraulic press pressure and the ratio of the piston areas of the hydraulic press and the squeezer.

Interstitial water was passed through a prewashed Whatman Number 1 filter above a titanium screen, filtered through a 0.45 µm Gelman polysulfone disposable filter (except for microbiology aliquots, which were drawn prior to Gelman filtration), and subsequently extruded into a 50 mL gas-tight glass syringe, a new sterile 50 mL plastic syringe, or an acid-cleaned and combusted glass vial. Both types of syringes were attached to the bottom of the squeezer assembly via a three-way plastic valve.

Distinct procedures were used to collect fluids for ^{14}C analysis and organic/microbial analyses. A 50 mL glass syringe was used to collect the first 50 mL from the squeezer for ^{14}C analysis. The remainder of the interstitial water from the squeezer was dispensed into a plastic syringe for shipboard and shore-based analyses. Samples for organic chemistry were extruded from the squeezer into plastic syringes and Gelman filter assemblies that were first rinsed with 18 MΩ deionized water; attempts were made to dry the syringe and filter before use. Incomplete drying was observed in the chlorinity data, and this rinsing procedure was stopped after Hole U1363C. After interstitial water was collected, the syringe was removed to dispense aliquots for shipboard and shore-based analyses.

Samples were stored in acid-cleaned plastic vials and bottles pending shipboard and shore-based analyses. Aliquots for shore-based trace metal and elemental analyses were placed in warm (60°C) HDPE plastic vials and acidified with 4 mL of subboiled 6N HCl per liter of sample. Aliquots for organic carbon, amino acids, and low molecular weight organic acids were stored in acid-cleaned combusted glass vials and frozen at –20°C. Aliquots for microbiology were either (1) transferred into cryovials, fixed with formaldehyde (3.7% final), and placed at 4°C before freezing at –80°C or (2) filtered onto a 0.1 µm Supor filter that was subsequently placed at the bottom of a 15 mL sterile plastic vial and covered in lysis buffer before freezing at –80°C (see **"Microbiology"**). Samples for ^{14}C analysis were placed in evacuated glass serum bottles (60 or 120 mL). These bottles contained 20 µL of saturated mercuric chloride that was evaporated before the bottle was evacuated.

Interstitial water samples were analyzed according to standard shipboard procedures (Gieskes et al., 1991). The pH was determined by ion-selective electrode. Alkalinity was determined by Gran titration with a Metrohm autotitrator. Chloride analysis was carried out by potentiometric titration using silver nitrate and a Mettler Toledo DL25 titrator equipped with a silver ring electrode (Mettler/Toledo ME 89599) with 2M KNO_3 electrode filling solution. All quantifications were based on comparison with International

Association for the Physical Sciences of the Ocean (IAPSO) standard seawater. Nutrients (phosphate and ammonium) were measured aboard ship using standard colorimetric methods. Sulfate and the major cations in seawater (Na, Ca, Mg, and K) were measured aboard ship using ion chromatography. Shore-based analyses include Na calculated by difference, Br measured using ion chromatography, major and minor ions measured using inductively coupled plasma–optical emission spectroscopy (ICP-OES) (Na, Mg, Ca, K, Sr, Li, B, Mn, Fe, Li, Si, and Ba), and some trace elements measured using inductively coupled plasma–mass spectroscopy (ICP-MS) with a sample dilution of 1:75 (U, V, Co, Rb, Mo, Cs, and Ba).

Because the nitrate data from shipboard samples showed evidence of contamination, additional pore water was extracted from the center of sediment whole-round samples that had been frozen at –80°C since collection. Whole-round samples were thawed overnight in a 4°C cold room, and ~50 cm^3 of sediment was removed from the interior, transferred to sterile 50 mL plastic tubes, and refrozen at –80°C. Precleaned acid-washed rhizon samplers were inserted into the remaining sediment interior (at least 5 cm sediment height) to collect pore water into 10 mL syringes via a three-way stopcock. The first 1 mL of collected pore water was flushed from the syringe to clean it. Once enough pore water was collected, the sample was transferred to a sterile 10 mL plastic tube and frozen at –20°C. These samples were analyzed using standard colorimetric methods (flow injection analysis) for nutrient analysis (ammonium, nitrate, and phosphate).

Microbiology

The primary microbiology objective for Expedition 327 was to determine the microbial community composition harbored in the buried basaltic oceanic crust at Sites U1362 (prospectus Site SR-2) and U1363 (prospectus Sites GRB-1, GRB-2, and GRB-3) on the Juan de Fuca Ridge flank. These studies expand on previous work in this region at nearby Site U1301 during IODP Expedition 301 and postexpedition in Holes 1026B, U1301A, and U1301B (Cowen et al., 2003; Engelen et al., 2008; Fisher et al., 2005; Lever et al., 2006; Nakagawa et al., 2006; Orcutt et al., 2011; Wheat et al., 2010). The secondary microbiology objective of this expedition was to collect sediment from Grizzly Bare outcrop (Site U1363) to examine the influence of presumed seawater recharge on sediment microbiology and to compare these findings with microbiological results obtained from sediments drilled during Expedition 301 (Engelen et al., 2008; Lever et al., 2010).

The microbiology strategy for Expedition 327 was to

- Collect deep basaltic crust from Hole U1362A,
- Collect upper oceanic crust from drill bit samples (when available),
- Collect sediment and upper basement from Grizzly Bare outcrop (Site U1363),
- Collect microbiological tracer samples during the 24 h pumping test in Hole U1362B, and
- Deploy new microbial colonization experiments downhole in the subseafloor borehole observatories ("CORKs") in Holes U1362A and U1362B.

This section focuses on the shipboard methods used for rock, sediment, and pore water sample collection and handling for microbiological analyses; CORK-related experiments are described in **Fisher, Wheat, et al.**; tracer experiment–related microbial activities are briefly described here and in more detail in **Fisher, Cowen, et al.** Briefly, samples of oceanic crust collected for microbiology were subsampled for environmental DNA extraction and analysis, cell counts, fluorescent in situ hybridization (FISH) studies, and contamination tests. Sediment samples were also collected for DNA extraction and analysis, cell counts, FISH, and contamination tests, and additional samples were collected to examine the potential for microbial dehalogenation metabolic activities.

Core handling and sampling

To examine potential contamination of hard rock and sediment core samples, slurries of yellow-green fluorescent microspheres (Fluoresbrite Carboxylate Microspheres; Polysciences, Inc., 15700) were sealed in plastic bags and placed inside the core catcher prior to deployment of the core barrel according to standard protocol (Smith et al., 2000a, 2000b). Perfluorocarbon tracer (PFT) contamination checks were not conducted during this expedition.

Hard rock cores

Hard rock samples for microbiology originated from RCB coring in Hole U1362A and APC/XCB coring at Grizzly Bare outcrop Site U1363. Priority was given to large (>10 cm in length) intact pieces or samples with interesting lithology. Nominally one sample was collected per section. Immediately following delivery of core on deck, rocks were exposed for subsampling in the core splitting room by either splitting the recovered core liner or shaking the recovered rocks into another split core liner (which,

because of frequent splitting blade breakage, was much faster than trying to split the recovered core liner). Rocks for microbiological sampling were identified immediately, photographed in place, and then collected using combusted aluminum foil for transport to the microbiology laboratory. All sample handlers wore gloves to reduce contamination. In the laboratory, rock pieces were transferred to a flame-sterilized rock processing box (Fig. F8) and broken into smaller pieces using flame-sterilized chisels and forceps. Subsampling was done as rapidly as possible (5–15 min) to minimize oxygen exposure and cell degradation. Care was taken to separate outer layers with higher potential for contamination. Rock fragments from the outer and inner layers were prepared and preserved for later microbiological analyses using one of the following methods:

1. Fixed in cold 3.7% [w/v] paraformaldehyde in 1× phosphate-buffered saline (PBS; 150 mM NaCl + 10 mM sodium phosphate, pH 7.2) for cell counts and FISH.
2. Transferred to a sterile plastic tube, covered with 3% formaldehyde, and then stored at 4°C for 4–6 h before filtration onto a 0.1 µm mesh black polycarbonate membrane.
3. Transferred to sterile sample bags and frozen immediately at –80°C.
4. Sprayed with ethanol and flamed to remove outer layers of contamination from the rock surface and then allowed to cool before being transferred to sterile sample bags and frozen at –80°C.
5. Covered with lysis buffer before being stored at –80°C.
6. Mixed with distilled water for microsphere contamination checks.

Leftover rock material was washed in deionized water, dried, and returned to shore-based laboratories for use as substrate in future colonization experiments.

Sediment cores

Sediments for microbiological analysis were collected as whole-round or syringe samples. APC and XCB cores were cut on the catwalk using sterilized tools (autoclaved spatulas and ethanol-cleaned and combusted foil-wrapped end caps), and all handlers wore gloves to minimize contamination. Prior to whole-round sample collection, cores were visually inspected for gas voids, cracks, or drilling disturbance. In Hole U1363B, roughly two microbiological sample sets were collected per sediment core throughout the entire sediment column. Samples were typically collected near the base of the core and also in Section 3, except near the sediment/basalt interface, where sampling frequency was higher. For each sample set in Hole U1363B,

1. Three to four whole-round samples (for shore-based DNA analysis, halogenated organic matter characterization, and incubation experiments) were taken next to an interstitial water sample, immediately capped with ethanol-cleaned end caps, and bagged for sample storage.
   a. Whole-round samples for shore-based DNA extraction and analysis and shore-based analysis of halogenated organics were immediately transferred to a sterile sample bag and frozen at –80°C.
   b. Whole-round samples for shore-based dehalogenation enrichment studies were capped, transferred into sealable gas-tight bags, and then impulse-sealed with anaerobic gas packs (BD BBL GasPak Plus) and stored cold (4°C).
2. Three syringe samples were collected (two interior and one exterior) from the whole-round core with sterile cut-end syringes for headspace analysis (one interior) and shore-based cell count and microsphere contamination analyses (one interior and one exterior). Samples for cell counts and microsphere contamination analyses were mixed with cold 3.7% [w/v] formaldehyde in 1× PBS (pH 7.4) for fixation.

Because of compressed coring schedules at the end of the cruise, microbiological sediment sample sets were compressed in Holes U1363C–U1363G to include only whole-round samples for shore-based DNA analysis and syringe samples for headspace and microsphere contamination checks (as described above) to allow for higher sampling frequency.

A subsample of the above cores was further sampled for parallel molecular diversity and organic geochemistry analyses. The outer perimeter and tops and bottoms of whole-round samples were removed with sterile scalpels that had also been rinsed with a methanol-methylchloride (1:1 v/v) solution. The remaining sample was then split into subsamples using a methanol-methylchloride–rinsed spatula for the following:

1. DNA extraction: subsamples were transferred to sterile 50 mL tubes, covered with lysis buffer, and frozen at –80°C.
2. Microscopy and FISH: samples were placed in similar 50 mL tubes, covered with 3.7% formaldehyde solution, and refrigerated at 4°C for several hours before being frozen at –80°C.
3. Lipid biomarker analyses: subsamples were transferred to a combusted glass jar, covered with a polytetrafluoroethylene-lined cap, and frozen at –80°C.

Splits of sediment pore water also were collected for microbial and organic analyses (see **"Pore water geochemistry"**). Whole-round samples were processed in a N_2-purged glove bag where their perimeters, tops, and bottoms were removed with clean spatulas. The remaining whole-round samples were placed in stainless steel press assemblies before being pressed under as much as 25,000 psi. However, for these samples the first 11 mL of pore water was collected into a sterile syringe under low pressure: 1 mL from this syringe was transferred directly to a 2 mL cryovial, and the remaining 10 mL was filtered through a 0.1 µm mesh Supor filter. Then, 90 µL of 37% formaldehyde was added to the cryovial, which was then stored at 4°C for several hours before being frozen at –80°C. The Supor filter was placed at the bottom of a sterile 15 mL tube, covered in lysis buffer, and frozen at –80°C. Other pore water aliquots were distributed among combusted glass scintillation vials for shore-based analysis of dissolved organic carbon, amino acids, and low molecular weight organic acids.

Hole U1362B tracer injection experiment microbiological sampling

A 24 h pumping and tracer injection experiment was performed in Hole U1362B as part of a large-scale, long-term multi-CORK tracer transport project. The rationale and injection and monitoring methods for this experiment are described elsewhere (**Fisher, Cowen, et al.**). The tracers used include (1) fluorescent microspheres of different sizes (0.5 and 1.0 µm) and surface charges (neutral or carboxyl) intended as stable proxies for microorganisms and (2) fluorescently stained (4′,6-diamindino-2-phenylindole [DAPI]) microorganisms concentrated from 63 µm strained surface seawater. Fluid sampling at the rig floor during the 24 h tracer injection was conducted to monitor the injection profile of fluorescent microspheres and DAPI-stained bacteria; these samples were then preserved for shore-based microscopy analysis for comparison with future colonization experiments to be recovered from the Hole U1362B CORK.

Storage and shipment conditions

All samples for shore-based DNA extraction and analysis and shore-based halogenated organic analysis were stored and shipped at –80°C, whereas samples for shore-based cell counts, FISH, and dehalogenation enrichment studies were stored and shipped cold (4°C).

Analytical methods

Cell counts and FISH

Samples for cell counts and FISH were fixed in cold 3.7% [w/v] formaldehyde in 1× PBS. After 1–4 h of fixation, a subsample was removed and washed twice with cold 1× PBS before being stored in 1:1 (v/v) 1× PBS:ethanol. This washed sample will be used for shore-based FISH analyses, whereas the unwashed sample will be used for cell counting with either SYBR Green I or acridine orange fluorescent dyes using previously described methods (Morono et al., 2009). On the basis of results from DNA extraction and analysis, microbial groups of interest will be investigated using group-specific FISH primers according to published protocols (Biddle et al., 2006).

DNA extraction and analysis

DNA will be extracted in shore-based laboratories using a variety of methods, depending on sample type. Genes of interest, including the 16S rRNA gene, as well as functional genes, will be amplified using the DNA extracts and polymerase chain reaction (PCR). PCR amplicons will then be cloned and sequenced to generate clone libraries following published protocols (Lever et al., 2010; Orcutt et al., 2011).

Dehalogenation analysis

Halogenated organics will be extracted from frozen sediments in a shore-based laboratory following published protocols (Covaci et al., 2007). Concentrations of compounds of interest will be quantified using a combination of coupled gas chromatography mass spectrometry, liquid chromatography, and gas chromatography. The potential for dehalogenation activities will be examined using sediment slurry enrichment incubations with compounds of interest in a shore-based laboratory, similar to previously used protocols (Futagami et al., 2009). The identity of potential dehalogenating microorganisms in sediment will be examined using group-specific 16S rRNA gene and functional gene analysis of DNA extracts in a shore-based laboratory.

Physical properties

Shipboard measurements of physical properties were performed to characterize the recovered material. Once cut to length, whole-round core sections were run through the WRMSL for measurement of gamma ray attenuation (GRA) density and magnetic susceptibility. The WRMSL also incorporates a compres-

sional wave velocity sensor (*P*-wave logger [PWL]) for sedimentary sections. PWL measurements were omitted for all hard rock cores, which rarely fill the core liner, resulting in velocity measurements that tend to be far less reliable than discrete sample data. Hard rock sections longer than 50 cm were measured with the NGRL, which is primarily intended to measure gamma rays resulting from the decay of ^{238}U, ^{232}Th, and ^{40}K isotopes.

After measurements with the WRMSL and NGRL were completed, thermal conductivity was measured on whole-round sediment cores using the needle probe method (Von Herzen and Maxwell, 1959). Thermal conductivity measurements on hard rock cores were made on pieces from the working halves using the half-space needle probe method (Vacquier, 1985).

Lastly, two discrete samples were usually taken from the working half of each section. Discrete samples were used for triaxial *P*-wave velocity measurements and moisture and density (MAD) measurements, including wet bulk density, dry bulk density, grain density, water content, and porosity. A comprehensive discussion of the methodologies and calculations used in the physical properties laboratory is presented in Blum (1997).

Whole-Round Multisensor Logger

GRA bulk density, magnetic susceptibility, and *P*-wave velocity were measured nondestructively with the WRMSL. Sampling intervals were set at 1 cm for hard rock and 2 cm for sediment, with an integration time of 5 s for each measurement of both types, which was determined to maximize the number and quality of measurements taken without slowing core flow. Quality assurance/quality control (QA/QC) was monitored by passing a core liner filled with freshwater through the WRSML after every core.

The primary objective of Expedition 327 was the recovery of hard rock from upper basaltic basement. In general, WRMSL measurements are most effective on a liner completely filled with core that has suffered minimal drilling disturbance. As a result, the diameter of the core liner (66 mm) is assumed for hard rock density calculations, even though the liner is often <100% filled. In addition, hard rocks are often recovered in pieces rather than as a continuous core, which reduces the actual volume even more. Therefore, GRA bulk density and magnetic susceptibility measurements tend to underestimate actual values for hard rock cores. *P*-wave velocities measured by the PWL suffer similar limitations and were thus measured only on sediment cores.

Gamma ray attenuation bulk density

The GRA densitometer on the WRMSL operates by passing gamma rays from a ^{137}Cs source down through a whole-round core into a 75 mm × 75 mm sodium iodide detector located directly below the core. Gamma rays with an energy peak at 662 keV are attenuated by Compton scattering as they pass through the core. The resultant gamma ray count is proportional to bulk density. Calibration of the GRA densitometer was performed using core liners filled with seawater and aluminum density standards. Recalibration was performed as needed if the freshwater QA/QC standard after every core deviated significantly (more than a few percent) from 1 g/cm^3. The spatial resolution of the GRA densitometer is <1 cm.

Magnetic susceptibility

Magnetic susceptibility, k, is a dimensionless measure of the degree to which a material can be magnetized by an external magnetic field:

$$k = M/H,$$

where M is the magnetization induced in the material by an external field strength H. Magnetic susceptibility responds to variations in the type and concentration of magnetic grains, making it useful for identifying compositional variations and alteration in hard rock cores. In the case of sediments, magnetic susceptibility can often be related to mineralogical composition (e.g., terrigenous versus biogenic material) and diagenetic overprinting (e.g., clays from the alteration of igneous materials have a susceptibility orders of magnitude lower than the material's original iron oxide constituents). Water and plastics (core liner) have a slightly negative magnetic susceptibility.

The WRMSL incorporates a Bartington Instruments MS2 meter coupled to an MS2C sensor coil with a diameter of 8.8 cm that operates at a frequency of 565 Hz. The sensor output can be set to centimeter-gram-second (cgs) units or SI units, with the IODP standard being the SI setting. The core diameter is smaller than the aperture through which it passes during measurement. Therefore, a volume-correction factor must be applied to the data off-line. Assuming a core diameter of 66 mm and using the coil aperture of 88 mm, the correction factor is found by multiplying the $\times 10^{-5}$ SI units by a factor of 0.68 (Blum, 1997).

The MS2C coil is calibrated with a homogeneous mixture of magnetite and epoxy in a 40 cm long piece of core liner to an accuracy of ±5%. The resolution of the method is ±4 cm for continuous core sec-

tion; therefore, magnetic susceptibility is underestimated for core material that is not continuous over an 8 cm interval.

P-wave logger

The WRMSL also includes a PWL, which was used to determine *P*-wave velocities in whole-round sediment cores. Specifics on the PWL and on other methods utilized to determine *P*-wave velocities are discussed in detail in **"*P*-wave velocity."**

Natural Gamma Radiation Logger

The NGRL was designed and built at IODP at Texas A&M University in order to augment geologic interpretations. Natural gamma rays occur primarily as a result of the decay of ^{238}U, ^{232}Th, and ^{40}K isotopes.

The main NGRL detector unit consists of 8 sodium iodide (NaI) scintillation detectors, 7 plastic scintillation detectors, 22 photomultipliers, and passive lead shielding. The NaI detectors are covered by 8 cm of lead shielding. In addition, lead separators (~7 cm of low-background lead) are positioned between the NaI detectors. The lead shielding closest to the NaI detectors is composed of low-background lead, whereas the outer half is composed of regular (virgin) lead. In addition to passive lead shielding, the NGRL detector unit employs a plastic scintillator to suppress the high-energy gamma and muon components of cosmic radiation by producing a veto signal when these charged particles pass through the plastic scintillators. The NGRL detector unit was calibrated using ^{137}Cs and ^{60}Co sources and identifying the peaks at 662 keV (^{137}Cs) and 1330 keV (^{60}Co).

Counts were summed over the range of 100–3000 keV to be compatible with data collection from previous cruises and for direct comparison with downhole logging data. Background measurements of an empty core liner counted for 40,000 s (11 h) were made before measuring Hole U1362A cores. Over the 100–3000 keV integration range, background counts averaged 3 counts per second, which often accounted for half or more of the overall signal.

A single NGRL run consisted of two sets of measurements by eight sensors, each spaced 20 cm apart. The two sets of measurements were offset 10 cm, which yielded a total of 16 measurements equally spaced 10 cm apart over a 150 cm long section of core. Cores less than 50 cm in length were not run through the NGRL.

The quality of the energy spectrum measured in a core depends on the concentration of radionuclides in the sample but also on the counting time, with higher times yielding more clearly defined spectra. Because of the low overall core yield, we had the opportunity to count for longer times (5400 s for each position [3 h total]), yielding statistically significant energy spectra for many cores.

Thermal conductivity

Thermal conductivity is the coefficient of proportionality relating conductive heat flow to a thermal gradient (Blum, 1997). Thermal conductivity was measured during Expedition 327 using the transient needle probe method in whole- or half-space geometry (Von Herzen and Maxwell, 1959), using a Teka Bolin TK04 system.

Half-space measurements were made with a needle probe embedded in the surface of an epoxy block having a low thermal conductivity (Vacquier, 1985). Samples were smoothed to ensure adequate contact with the heating needle. Visible saw marks were removed when necessary by grinding and polishing the split face using 120–320 gauge silicon carbide. In addition, a MACOR ceramic standard with a certified thermal conductivity of 1.637 ± 0.033 W/(m·K) was run repeatedly to verify instrument performance.

Half-space samples were equilibrated to room temperature in a seawater saturator for 12 h, and the samples and sensor needle were equilibrated together in an insulated seawater bath for at least 15 min prior to measurement. Isolation of the sample and sensor needle eliminated the effect of rapid but small temperature changes introduced by air currents in the laboratory. The instrument measures drift internally and does not begin a heating run until sufficient thermal equilibrium is attained. Samples were selected at irregular intervals (nominally one measurement per section) depending on the availability of homogeneous and relatively vein- and crack-free pieces long enough to be measured without edge effects (i.e., longer than the instrument needle, or 8 cm). Measurements were made at room temperature and pressure and were not corrected for in situ conditions. In practice, the shipboard thermal conductivity system was found to be unreliable for half-space measurements of hard rock during Expedition 327 because of a combination of hardware instability and the inflexibility of the acquisition and processing software. After many hours of effort debugging and crafting work-arounds for the system, evaluation of hard rock thermal conductivity was abandoned after collection of reliable data from only three samples.

For sediment cores, thermal conductivity was measured prior to the cores being split using the needle probe method in full-space configuration for soft sediments (Von Herzen and Maxwell, 1959). The needle probe was inserted into the unconsolidated sediment through 2 mm holes drilled into the core

liner roughly once per section, generally in locations determined using magnetic susceptibility data gathered on the WRMSL. In general, magnetic susceptibility is higher in sandier intervals and lower in clay-rich intervals. Both kinds of intervals were targeted in order to assess thermal conductivity within these end-members so that later analyses could assess thermal conductivity within intervals having a mixed lithology.

Section Half Multisensor Logger

Magnetic susceptibility

Magnetic susceptibility was measured with a Bartington Instruments MS2E point sensor on the SHMSL. Because the SHMSL demands flush contact between the magnetic susceptibility point sensor and the split core, measurements were made on the archive halves of split cores that were covered with clear plastic wrap. A built-in laser surface analyzer aided in the recognition of irregularities in the split-core surface (e.g., cracks and voids), and data from this tool were recorded to provide an independent check on the fidelity of SHMSL measurements (e.g., Expedition 301 Scientists, 2005b).

Color reflectance

Reflectance spectroscopy and colorimetry data were collected using an OceanOptics spectrophotometer (model USB4000) to provide a high-resolution stratigraphic record of color variations at Site U1363. These data are displayed in the Site U1363 visual core descriptions in **"Core descriptions."**

The SHMSL skips empty intervals and intervals where the core surface is well below the level of the core liner, but it does not recognize relatively small cracks or disturbed areas of core. Thus, SHMSL data may contain spurious measurements that should, to the extent possible, be edited out of the data set before use. The OceanOptics spectrophotometer measures the spectra from 380 to 900 nm at 2 nm bins. Data were captured at a measurement spacing of 1 cm using the L*a*b* color system based on a CIE D65 Standard Illuminant and 10-2 degree Standard Observer.

Moisture and density

Several basic physical properties of interest (bulk density, dry density, grain density, porosity, and void ratio) are found most accurately through mass and volume determinations on discrete samples. MAD data are also used for comparison with GRA bulk density data from the WRMSL. The shipboard MAD facility consists of a vacuum water saturator (for hard rock), a dual balance system for mass measurements, and a pycnometer for volume measurements.

In soft sediments, ~10 cm^3 samples were extracted—usually from the same locations as thermal conductivity measurements—and placed in preweighed 16 mL Wheaton beakers. Stiff sediments drilled with the XCB were sampled, where appropriate, by extracting ~10 cm^3 blocks using a spatula and placing the blocks into beakers, as above. One sample was routinely collected from each undisturbed section, and three to four samples per core were collected where recovery was good and sedimentation rates were high. Additional samples were taken where major changes in lithology were observed.

In hard rock sections, discrete samples were cut from the working halves of split cores at a nominal frequency of two samples per section. Cube-shaped samples, which were also used to measure *P*-wave velocities in three orthogonal directions, were extracted from oriented pieces. Cylinder-shaped samples were extracted from unoriented pieces. These ~7 cm^3 samples are intended to represent the general variation and lithologies of the core. Therefore, samples were collected when there was a visible change in lithology or texture.

Vacuum water saturator

Determination of a precise and accurate wet mass of sparsely porous material requires that the pore space of the sample be completely saturated. Hard rock samples were saturated prior to measurement using a vacuum pump system. The system consisted of a plastic chamber filled with seawater into which samples were placed. A vacuum pump removed air from the chamber, forcing seawater into the sample pore spaces. The samples were kept under vacuum for at least 12 h, after which the vacuum was checked at 2–3 h intervals to ensure a stable underpressure condition. After removal from the saturator, the cubes were stored in sample containers filled with seawater to prevent the evaporation of pore water. After *P*-wave velocity measurements, the cube surfaces were lightly patted with a paper towel to remove water clinging to the outer surfaces, and wet mass was immediately determined using the dual balance system.

Dual balance system

The dual balance system was used to measure both wet and dry masses. Two Mettler-Toledo XS204 analytical balances compensated for ship motion; one acted as a reference, and the other measured the unknown sample. A standard weight similar to that of the sample was placed on the reference balance to

increase accuracy. The default setting of the balances is 300 measurements (taking ~1.5 min to measure), which was deemed sufficient because no measurements were taken in transit.

Pycnometer system

The pycnometer system was used to measure dry sample volume using pressurized helium-filled chambers. At the start of the expedition and whenever the helium gas tank was changed, shipboard technicians performed a calibration using stainless steel spheres of known volume. A batch of samples consisted of four cells with unknowns and one cell with two stainless steel spheres (3 and 7 cm^3). The spheres were cycled through the cells to identify any systematic error or instrument drift. Spheres are assumed to be known within 1% of their total volume. Individual volume measurements were preceded by three purges of the sample chambers with research-grade (99.995% or better) helium heated to 25°C.

Measurement of wet mass and dry mass by the dual balance system, along with dry volume measured by the pycnometer, allows for the determination of a number of MAD properties. The MAD Method C in Blum (1997) was used to determine dry volumes by gas pycnometry.

P-wave velocity

P-wave velocity varies with the material's lithology, porosity, bulk density, state of stress, temperature, and fabric or degree of fracturing. Together with bulk density, velocity data are used to derive porosities and to calculate acoustic impedance, which can be used to construct synthetic seismograms and estimate the depths of seismic horizons.

Sediment

P-wave velocities of sediments were measured with the PWL on the WRMSL and with the *P*-wave caliper (PWC) and *P*-wave bayonets (PWB). The PWL measures the ultrasonic *P*-wave velocity of the whole-round sample in the core liner. The PWC and PWB measure *P*-wave velocity in a Cartesian coordinate system on section halves. The PWC measures *P*-wave velocity vertically to the sectional plane of the working half (horizontal direction; *x*-axis), whereas the PWB measures the cross section (horizontal direction; *y*-axis) and long axis (vertical direction; *z*-axis) of the core. We used the PWC only for lithified sediments because the cracks induced by the bayonets on the PWB precluded the acquisition of reliable velocities.

All tools transmit a 500 kHz *P*-wave pulse through the core section at a specified repetition rate. This signal is coupled to the sample by the plastic pole pieces of the transducers and by the pressure applied by the linear actuator. In contrast to the PWC and PWB, no water is used to improve coupling between the transducers of the PWL and the liner because the pressure applied by the actuator is sufficient for reliable *P*-wave measurement. In the PWL measurement, the wave propagation direction is perpendicular to the section's long axis (horizontal direction).

Traveltime was determined by signal-processing software that automatically detects the arrival of the *P*-wave signal to a precision of 50 ns. A linear voltage differential transformer was used to measure the separation of the transducer to derive a travel path length for the signal (i.e., the slightly compressed core diameter). Ultrasonic *P*-wave velocity was then calculated after corrections were made for system propagation delay, liner thickness, and liner material velocity.

Hard rock

P-wave velocity measurements of basaltic samples were performed on the same discrete samples (cube and cylinder samples) used for MAD measurements. Because discontinuous samples completely attenuate the signal, it is not possible to obtain continuous data from the PWL on the WRMSL. Sample preparation included cutting cubes and cylinders with flat and parallel sides. Using the Buehler Petrothin thin section system (240 grit), all surfaces of the samples were polished to ensure good contact between the sample and transducer.

P-wave velocity measurements were performed on seawater-saturated samples directly before wet mass determinations because *P*-wave velocity is very sensitive to the degree of saturation (Knight and Nolen-Hoeksema, 1990). Measurements used the *x*-axis caliper-type contact probe transducers (PWC). Oriented cube samples were rotated manually to measure *y*- and *z*-axis velocities with the same instrument. Deionized water was applied to the contact between the transducers and sample in order to improve acoustic coupling. The system uses Panametrics-NDT Microscan delay line transducers, which transmit a 500 kHz *P*-wave pulse. Although 500 kHz pulse generator and transducers were used, waveforms with ~110 kHz dominant frequency were obtained.

The estimated *P*-wave velocities are significantly higher than the expected velocity of basalt. Therefore, all saturated samples were measured, and the velocity of calibration standards was checked after every measurement. When the acrylic standard velocity calculated during every measurement was not within tolerances (2750 ± 20 m/s), the measurement device was calibrated with a series of acrylic cylin-

ders of differing thicknesses until the values converged. The velocity measurement device was usually calibrated after roughly every four velocity measurements. Because the estimated *P*-wave velocities were not stable, the velocities were measured four times on each axis by rotating every 90° and averaging the results.

After all velocity measurements were completed, velocities were recalculated for several discrete samples. Even though the measurement device was frequently recalibrated, the velocities differed from each other (±100 m/s difference). To check the accuracy of the velocity values, *P*-wave velocities were further calculated in dry conditions. *P*-wave velocities in dry conditions are usually slower than those in saturated conditions.

In the automatic picking procedure, the first positive peak was picked for traveltime determination. However, because the arrival time of the first positive peak is affected by sample attenuation and reflections, the first arrival (first break) of the waveforms was also picked. To pick the first arrival of the *P*-wave signal, waveforms were recorded for all samples in saturated and dry conditions. A reference waveform (i.e., waveform without a sample) was also calculated for every sample measurement. Traveltime (time lag between recorded waveform and reference waveform) was then obtained by displaying and correlating these waveforms (Fig. **F9**). Although the *P*-wave velocity collected by this method is a little slower (~150 m/s) than the velocity estimated via the conventional automatic picking method, the overall velocity trends derived from the two methods are consistent.

Paleomagnetism

The objectives of the paleomagnetic studies program during Expedition 327 were to measure paleomagnetic directions for tectonic and polarity studies and to examine magnetic properties on a regional scale by comparing the results with those of Expedition 301. Measurements were made on the archive-half sections of cores.

Paleomagnetic instruments

A 2G Enterprises pass-through cryogenic direct-current superconducting quantum interference device (SQUID) rock magnetometer (model 760R) was used to make paleomagnetic measurements. This magnetometer is equipped with an in-line alternating-field (AF) demagnetizer (2G model 2G600) that allows for demagnetization of samples up to 80 mT. The magnetometer and AF demagnetizer are interfaced with a workstation that is used to collect the data. The magnetization of the core liner sets the resolution of the instrument to ~3 × 10^{-5} A/m, but all samples had magnetization intensities above this limit.

The magnetic susceptibility of core sections was measured with two devices. Whole-round sections were measured on the WRMSL (see **"Physical properties"**). Section halves were measured on the SHMSL (see **"Physical properties"**).

Paleomagnetic measurements

Standard IODP orientation conventions were applied to the archive halves of the core (+*x*: vertically upward; +*y*: horizontally to the right when looking downcore; and +*z*: downcore) (Fig. **F10**).

The natural remanent magnetization (NRM) of samples was measured initially, followed by the magnetization after progressive AF demagnetization. Measurements were made on oriented pieces and along core sections that were not excessively fractured. Measurements were made using superconducting rock magnetometer (SRM) Discrete and SRM Section software. Hard rocks were demagnetized at 5 mT steps from 0 to 30 mT, with two additional steps at 40 and 50 mT. Hard rock pieces measured in discrete mode were positioned so that a single measurement was made at their center points. Hard rock pieces measured in section mode were sampled at 1 cm intervals. Because of orientation differences in how data were collected with the two applications, the *y* and *z* magnetic moments stored in the database of hard rock discrete pieces must be reversed before data generated by the two different measurement modes can be compared. Sediments were demagnetized at 10, 20, 30, and 40 mT steps and measured at 5 cm intervals.

Characteristic remanent magnetization directions (i.e., the magnetization believed to be that acquired initially upon cooling of the igneous flows) were determined by examining orthogonal vector plots of demagnetization steps and looking for a consistent direction of decay toward the origin. The mean directions of these vectors were calculated using principal component analysis (Kirschvink, 1980).

Geomagnetic polarity timescale

Magnetic polarity results were correlated to the polarity reversal sequence and absolute age using the Berggren et al. (1995) geochronology (Fig. **F11**). This timescale incorporates the widely used calibration of age and polarity intervals derived by Cande and Kent (1995).

Downhole measurements

Downhole measurements are used to determine the physical, chemical, and structural properties of the formation penetrated by a borehole. Wireline logging data are collected rapidly and continuously with depth and are measured in situ; they can be interpreted in terms of the stratigraphy, lithology, mineralogy, and geochemical composition of the penetrated formation. Where core recovery is incomplete or disturbed, these data may provide the only way to characterize the continuous borehole section. Where core recovery is good, log and core data complement one another and may be interpreted jointly. Wireline logs measure formation properties on a scale that is intermediate between those obtained from laboratory measurements on core samples and those obtained during geophysical surveys. They are useful in calibrating the interpretation of geophysical survey data and provide a necessary link for the integrated understanding of physical properties on all scales.

Sediment temperature measurements are used to assess thermal conditions at depth, both within sediments and in the underlying volcanic crust. These sediment temperature measurements cannot be made remotely from a surface ship but require drill string deployment of tools within sediment at the bottom of a borehole. The same tools can be deployed in the open hole, but measurements there may be disturbed by flowing water or the thermal influence of recent drilling and other operations.

Wireline logging

Data are recorded during wireline logging operations by a variety of Schlumberger and third-party tools. These tools can be combined in many configurations and run into the borehole after drilling or coring operations are completed. A single wireline tool string was used to log Hole U1362A during Expedition 327 (Fig. **F12;** Table **T4**). The tool string contained a telemetry cartridge for communicating through the wireline to the Schlumberger data acquisition system on the drillship.

The wireline tools used and their measurement principles are briefly described below. The main measurements are listed in Table **T4.** More detailed information on individual tools and their geological applications may be found in Ellis and Singer (2007), Goldberg (1997), Lovell et al. (1998), Rider (1996), Schlumberger (1989), and Serra (1984, 1986). Acronyms and units for wireline measurements are listed in Table **T5.** An online list of acronyms for Schlumberger tools and measurement curves is available in the Documents section of the Expedition 327 log database (**brg.ldeo.columbia.edu/data/iodp-usio/exp327/U1362A/**). In the following sections, tools deployed during Expedition 327 are described, working upward from the bottom of the tool string.

Ultrasonic Borehole Imager

The Schlumberger Ultrasonic Borehole Imager (UBI) features a high-resolution transducer that provides acoustic images of the borehole wall. The transducer emits ultrasonic pulses at a frequency of 250 or 500 kHz (low and high resolution, respectively); these pulses are reflected at the borehole wall and then received by the same transducer. The amplitude and traveltime of the reflected signal are determined. The continuous rotation of the transducer and the upward motion of the tool produce a complete map of the borehole wall. The amplitude depends on the reflection coefficient of the borehole fluid/rock interface, the position of the UBI tool relative to the center of the borehole, the shape of the borehole, and the roughness of the borehole wall. Changes in borehole wall roughness (e.g., at fractures intersecting the borehole) are responsible for the modulation of the reflected signal; this makes it possible for fractures or other variations in the character of the drilled rocks to be recognized in the amplitude image. The recorded traveltime image gives detailed information about the shape of the borehole and allows calculation of a borehole caliper value from each recorded traveltime.

Amplitude and traveltime are recorded together with a reference to magnetic north by means of the General Purpose Inclinometry Tool (GPIT), permitting image orientation. If features (e.g., fractures) recognized in the core are observed in the UBI images, core orientation is possible. UBI-oriented images can also be used to measure stress in the borehole through identification of borehole breakouts and slip along fault surfaces penetrated by the borehole (Paillet and Kim, 1987).

General Purpose Inclinometry Tool

Three-axis acceleration and magnetic field measurements were made with the Schlumberger GPIT. The primary purpose of this tool is to determine the acceleration and orientation of the UBI tool during logging. Images are corrected for irregular tool motion caused by the drillship's heave and can be oriented for accurate determination of the dip and direction of features. The GPIT's vertical acceleration data are also used to calculate downhole tool motion, which in turn is used to evaluate the wireline heave compensator (WHC).

Modular Temperature Tool

The Lamont-Doherty Earth Observatory (LDEO) Modular Temperature Tool (MTT) measures borehole fluid temperature using a resistance-temperature device. Along with acceleration, this temperature is sent in real time to the surface using Schlumberger telemetry.

Hostile Environment Litho-Density Sonde

Formation density was determined with the Schlumberger Hostile Environment Litho-Density Sonde (HLDS). The sonde contains a radioactive cesium (^{137}Cs) gamma ray source (622 keV) and far and near gamma ray detectors mounted on a shielded skid, which is pressed against the borehole wall by a hydraulically activated eccentralizing arm. Gamma rays emitted by the source undergo Compton scattering, which involves the transfer of energy from gamma rays to the electrons in the formation via elastic collision. The number of scattered gamma rays that reach the detectors is directly related to the density of electrons in the formation, which is in turn related to bulk density. Porosity may also be derived from this bulk density if the matrix (grain) density is known.

The HLDS also measures photoelectric absorption as the photoelectric effect (PEF). Photoelectric absorption of the gamma rays occurs when their energy is reduced below 150 keV after being repeatedly scattered by electrons in the formation. Because PEF depends on the atomic number of the elements in the formation, it also varies according to the chemical composition of the minerals present. The use of drilling mud containing barite can significantly affect PEF measurements.

Hostile Environment Natural Gamma Ray Sonde

The Schlumberger Hostile Environment Natural Gamma Ray Sonde (HNGS) uses two bismuth germanate scintillation detectors and five-window spectroscopy to provide measurements of total gamma ray and to determine the concentrations of isotopes that dominate the natural radiation spectrum: ^{40}K, ^{232}Th, and ^{238}U.

Logging equipment head

The Schlumberger logging equipment head (LEH), or cable head, measures tension at the top of the wireline tool string, which helps diagnose difficulties running the tool string up or down the borehole or when exiting or entering the drill string or casing. A spontaneous potential (SP) electrode was installed in the LEH to record a qualitative SP log of the borehole. Developed for wells drilled into sediment formations on land, the SP method is traditionally a measure of the slight electric potential difference between an electrode in the logging tool and one grounded at the surface. This potential difference normally results from the flow of conductive water through formations and the charge separation of clay near the borehole wall. The absolute value of the SP curve is meaningless: only the curve deflection is of interest. During Expedition 327, SP measurements did not use a surface electrode or fish; instead SP is a measure of the potential difference between the LEH electrode and the wireline cable grounded to the drillship. The SP measurement is further impaired by stray current at the rig and by the comparable salinities of the drilling fluid (seawater) and formation water.

Wireline log data quality

The principal influence on log data quality is the diameter of the borehole and the condition of the borehole wall. If the borehole diameter is large or if it is rugose or variable over short intervals because of washouts during drilling or ledges caused by layers of harder material, the HLDS logs may be degraded. Deep investigation measurements, such as gamma ray, that do not require contact with the borehole wall are generally less sensitive to borehole conditions. Very narrow ("bridged") sections also cause irregular log results. Borehole quality is improved by minimizing fluid circulation while drilling, flushing the borehole to remove debris, and logging as soon as possible after drilling and conditioning are completed.

The quality of depth determination depends on a series of factors. The depth of the logging measurements is determined from the length of the logging cable played out at the winch on the ship and from calculation of cable stretch. The seafloor is identified on the natural gamma log by the abrupt reduction in gamma ray count at the water/sediment interface (mudline). Discrepancies between driller's depth and wireline log depth can occur because of core expansion, incomplete core recovery, tidal variation, incomplete heave compensation, and drill pipe stretch in the case of driller's depth. In the case of log depth, error is introduced because of incomplete heave compensation, incomplete correction for cable stretch, and cable slip. To minimize wireline tool motion caused by ship heave, a hydraulic WHC adjusts for rig motion during wireline logging operations.

Logging data flow and processing

Data for each wireline logging run were monitored in real time and recorded using the Schlumberger

MAXIS system. Immediately after logging, field prints were made and shared with the science party. Simultaneously, the data were transferred on shore to the Borehole Research Group at LDEO for standardized data processing. There, data were depth shifted, corrections were made to the UBI images, documentation for the logs was prepared, and the data were converted to ASCII for the conventional logs and GIF for the UBI images. The Schlumberger GeoFrame reservoir characterization software package was used for most of the processing. The data were transferred back to the ship within a few days of logging and made available (in ASCII and digital log interchange standard [DLIS] formats) through the shipboard IODP log database.

The initial logging data are referenced to the rig floor (WRF). After logging was completed, the data were shifted to a seafloor reference (WSF) on the basis of the step in gamma radiation and caliper deflection at the casing shoe, and ultimately all data were shifted to a single reference pass, yielding the WMSF scale.

In situ temperature measurements

The Expedition 327 downhole measurements program included deployment of three kinds of temperature tools that were used to help determine heat flow within sediments and assess the thermal state of the borehole. Measurements within sediments should provide an indication of predrilling thermal conditions because the temperature tools penetrate ahead of the bit into undisturbed material. In contrast, measurements in boreholes can be strongly influenced by drilling operations, particularly if made soon after drilling. Borehole thermal data in basement are potentially useful, nevertheless, because they can indicate formation intervals that are likely to be hydrogeologically active. In addition, temperature measured in a sealed borehole, such as one isolated by a CORK, provide useful information on ambient borehole conditions and the thermal state of the surrounding formation.

Advanced piston corer temperature tool

The third-generation advanced piston corer temperature tool (APCT-3) is an instrumented version of the coring shoe that is run during APC coring. It is deployed in soft sediments to obtain formation temperatures to determine the geothermal gradient.

The APCT-3 does not require a separate tool run but is deployed on an APC inner core barrel and provides an in situ temperature measurement while adding 15–20 min to the core barrel run. The tool is lowered with the core barrel down the drill string by coring line and then held just above the seafloor for 10 min to measure bottom water temperature. The shoe is lowered into the bit and hydraulically stroked into the sediment (~9.5 m ahead of the bit for a normal deployment) and remains stationary while temperature data are recorded for 7–8 min. The APC inner core barrel is retrieved, the instrumented shoe is removed, and the data are downloaded into a computer. Processing requires extrapolating the frictional decay curve to determine in situ temperature by fitting the data to a theoretical model (Heesemann et al., 2006).

Sediment Temperature tool

The Sediment Temperature (SET) tool is designed to take heat flow measurements in semiconsolidated sediments that are too stiff for the APCT-3. Coring must be interrupted to take a SET temperature measurement: the tool is lowered into the borehole on a dedicated coring line, generally with a brief pause just above the seafloor to measure the bottom water temperature. The SET is typically run with the colleted delivery system, which latches into the bottom-hole assembly (BHA). The tool's probe extends 1.4 m below the bit and is pushed into undisturbed bottom sediment by the driller. The colleted delivery system allows the probe to be disengaged from the BHA, which helps to reduce disturbance from drill string movement while the probe is in the sediment. The probe is typically held in the sediment for 10 min and then returned to the surface, where its data are downloaded for analysis. As with the APCT-3, SET data are analyzed by fitting observations to an idealized model incorporating tool geometry and sediment properties.

Miniaturized temperature data logger

After the original instrument string was removed from the CORK in Hole U1301B, two custom-modified ANTARES type 1857 miniaturized temperature data loggers (MTLs) were encased in a perforated protective pipe below a sinker bar and lowered on the coring line into the borehole. The coring line was stopped for ~5 min at 5 m intervals in the uppermost 50 m of the hole and for 5 min every 25 m thereafter to register a downhole temperature profile. The MTLs recorded temperature with a resolution of 0.001°C. The loggers were calibrated in 2009 and were accurate to 0.002°C.

Hydrologic experiments

Drill string packer experiments

A drill string packer was used during Expedition 327 to isolate and test the hydrological properties of the

basement section in Hole U1362A. The tools and methods employed were similar to those developed and applied during ODP, especially as described for ODP Legs 139 (Shipboard Scientific Party, 1992b) and 168 (see Appendix of Becker and Fisher, 2000). In summary, the method involves

1. Activating the inflatable element of the packer to isolate the formation to be tested;
2. Using the rig mud pumps to pump seawater into the isolated formation in a controlled fashion, either as short (<1 min) pressure impulses for "slug tests" or at a constant rate for "injection tests" lasting tens of minutes to hours; and
3. Recording the pressure response in the isolated zone and at the rig floor standpipe.

The pressure records can be interpreted to estimate the average or bulk permeability of the isolated zone close to the borehole.

The methods used in previous *JOIDES Resolution* packer operations were modified and improved during Expedition 327 as follows. A new generation of electronic pressure gauges was used to record both downhole pressures in the isolated zone and rig floor pressures at the standpipe. Downhole pressures were recorded with 0–10,000 psi Micro-Smart HT-750 gauges having a programmable sampling rate and memory capacity for up to 500,000 data points. These gauges are much smaller than those used in previous ODP/IODP packer experiments, and they were deployed in a newly designed gauge carrier attached to the go-devil that enables packer inflation. Pressures at the rig floor were recorded at comparable sampling rates by the standard Rig Instrumentation System standpipe pressure gauge. Injection test duration was also extended. Following Expedition 301 procedures, we expected to run injection tests on the order of 1–2 h, longer than the typical 20–30 min tests conducted during ODP.

24 h tracer injection/hydrologic experiment

A long-term tracer injection test unlike any previously conducted on the *JOIDES Resolution* was run in Hole U1362B in order to assess rates and patterns of fluid flow in basement and to quantify basement hydrogeologic properties across a range of spatial scales (**Fisher, Cowen, et al.**). This test was conducted after the new CORK was installed in Hole U1362A. This test included 24 h of continuous injection (at a nominal injection rate of 5–7 L/s), with the addition of multiple tracers, to produce pressure, chemical, and microbial signals to be monitored with instruments deployed in Hole U1362B, and with gauges and fluid samplers deployed earlier in nearby CORKs in Holes 1026B, 1027C, U1301A, U1301B, and U1362A. Because the inflatable drill string packer is subject to deflation on large heaves and relies on friction between the packer element and the borehole or casing wall to hold position, we ran the 24 h hydrologic experiment in Hole U1362B using a casing running tool in lieu of a drill string packer. The casing running tool was lowered into the throat of the reentry cone and then set down such that it was held mechanically by the 10¾ inch casing hanger and sealed by an O-ring between the running tool and hanger. This configuration allowed use of the same downhole pressure gauges used in the drill string packer experiments, in addition to multiple high-rate OsmoSamplers that were placed in a newly designed carrier system positioned at the end of a stinger that extended just beyond the end of the 10¾ inch casing. During Expedition 327, only data from the instruments in Hole U1362B were available because pressure data and fluid samples in the nearby CORKs will not be recovered until CORK servicing in summer 2011 or 2012.

The tracers used for the 24 h injection experiment comprised freshwater (alternated with seawater); SF_6 (an inert gas); the salts CsCl, $ErCl_3$, and $HoCr_3$; fluorescent microspheres of several sizes and excitation wavelengths; and fluorescent-stained bacterial cells (strained from surface seawater). Different tracers were injected using different methods throughout the 24 h hydrologic experiment, as discussed in **Fisher, Cowen, et al.**

References

Becker, K., and Fisher, A.T., 2000. Permeability of upper oceanic basement on the eastern flank of the Juan de Fuca Ridge determined with drill-string packer experiments. *J. Geophys. Res., [Solid Earth],* 105(B1):897–912. **doi:10.1029/1999JB900250**

Berggren, W.A., Kent, D.V., Swisher, C.C., III, and Aubry, M.-P., 1995. A revised Cenozoic geochronology and chronostratigraphy. *In* Berggren, W.A., Kent, D.V., Aubry, M.-P., and Hardenbol, J. (Eds.), *Geochronology, Time Scales, and Global Stratigraphic Correlation.* Spec Publ.—SEPM (Soc. Sediment. Geol.), 54:129–212. **doi:10.2110/pec.95.04.0129**

Biddle, J.F., Lipp, J.S., Lever, M.A., Lloyd, K.G., Sørensen, K.B., Anderson, R., Fredricks, H.F., Elvert, M., Kelly, T.J., Schrag, D.P., Sogin, M.L., Brenchley, J.E., Teske, A., House, C.H., and Hinrichs, K.-U., 2006. Heterotrophic Archaea dominate sedimentary subsurface ecosystems off Peru. *Proc. Natl. Acad. Sci. U. S. A.,* 103(10):3846–3851. **doi:10.1073/pnas.0600035103**

Blum, P., 1997. Physical properties handbook: a guide to the shipboard measurement of physical properties of deep-sea cores. *ODP Tech. Note,* 26. **doi:10.2973/odp.tn.26.1997**

Cande, S.C., and Kent, D.V., 1995. Revised calibration of the geomagnetic polarity timescale for the Late Creta-

ceous and Cenozoic. *J. Geophys. Res., [Solid Earth],* 100(B4):6093–6095. **doi:10.1029/94JB03098**

Covaci, A., Voorspoels, S., Ramos, L., Neels, H., and Blust, R., 2007. Recent developments in the analysis of brominated flame retardants and brominated natural compounds. *J. Chromatogr., A,* 1153(1–2):145–171. **doi:10.1016/j.chroma.2006.11.060**

Cowen, J.P., Giovannoni, S.J., Kenig, F., Johnson, H.P., Butterfield, D., Rappé, M.S., Hutnak, M., and Lam, P., 2003. Fluids from aging ocean crust that support microbial life. *Science,* 299(5603):120–123. **doi:10.1126/science.1075653**

Ellis, D.V., and Singer, J.M., 2007. *Well Logging for Earth Scientists,* (2nd ed.): Dordrecht, The Netherlands (Springer).

Engelen, B., Ziegelmüller, K., Wolf, L., Köpke, B., Gittel, A., Cypionka, H., Treude, T., Nakagawa, S., Inagaki, F., Lever, M.A., and Steinsbu, B.O., 2008. Fluids from the ocean crust support microbial activities within the deep biosphere. *Geomicrobiol. J.,* 25(1):56–66. **doi:10.1080/01490450701829006**

Expedition 301 Scientists, 2005a. Methods. *In* Fisher, A.T., Urabe, T., Klaus, A., and the Expedition 301 Scientists, *Proc. IODP,* 301: College Station, TX (Integrated Ocean Drilling Program Management International, Inc.). **doi:10.2204/iodp.proc.301.105.2005**

Expedition 301 Scientists, 2005b. Site U1301. *In* Fisher, A.T., Urabe, T., Klaus, A., and the Expedition 301 Scientists, *Proc. IODP,* 301: College Station, TX (Integrated Ocean Drilling Program Management International, Inc.). **doi:10.2204/iodp.proc.301.106.2005**

Expedition 309/312 Scientists, 2006. Methods. *In* Teagle, D.A.H., Alt, J.C., Umino, S., Miyashita, S., Banerjee, N.R., Wilson, D.S., and the Expedition 309/312 Scientists. *Proc. IODP,* 309/312: Washington, DC (Integrated Ocean Drilling Program Management International, Inc.). **doi:10.2204/iodp.proc.309312.102.2006**

Fisher, A.T., Wheat, C.G., Becker, K., Davis, E.E., Jannasch, H., Schroeder, D., Dixon, R., Pettigrew, T.L., Meldrum, R., McDonald, R., Nielsen, M., Fisk, M., Cowen, J., Bach, W., and Edwards, K., 2005. Scientific and technical design and deployment of long-term subseafloor observatories for hydrogeologic and related experiments, IODP Expedition 301, eastern flank of Juan de Fuca Ridge. *In* Fisher, A.T., Urabe, T., Klaus, A., and the Expedition 301 Scientists, *Proc. IODP,* 301: College Station, TX (Integrated Ocean Drilling Program Management International, Inc.). **doi:10.2204/iodp.proc.301.103.2005**

Futagami, T., Morono, Y., Terada, T., Kaksonen, A.H., and Inagaki, F., 2009. Dehalogenation activities and distribution of reductive dehalogenase homologous genes in marine subsurface sediments. *Appl. Environ. Microbiol.,* 75(21):6905–6909). **doi:10.1128/AEM.01124-09**

Gieskes, J.M., Gamo, T., and Brumsack, H., 1991. Chemical methods for interstitial water analysis aboard *JOIDES Resolution. ODP Tech. Note,* 15. **doi:10.2973/odp.tn.15.1991**

Goldberg, D., 1997. The role of downhole measurements in marine geology and geophysics. *Rev. Geophys.,* 35(3):315–342. **doi:10.1029/97RG00221**

Govindaraju, K., 1989. 1989 compilation of working values and sample description for 272 geostandards. *Geostand. Newsl.,* 13(S1). **doi:10.1111/j.1751-908X.1989.tb00476.x**

Heesemann, M., Villinger, H., Fisher, A.T., Tréhu, A.M., and White, S., 2006. Data report: testing and deployment of the new APCT-3 tool to determine in situ temperatures while piston coring. *In* Riedel, M., Collett, T.S., Malone, M.J., and the Expedition 311 Scientists. *Proc. IODP,* 311: Washington, DC (Integrated Ocean Drilling Program Management International, Inc.). **doi:10.2204/iodp.proc.311.108.2006**

Hunt, J., Wynn, R.B., Masson, D.G., and Croudace, I.W., 2010. Geochemical evidence of multistage retrogressive failure during the 160,000 ka Icod landslide from turbidite facies analysis: multidisciplinary investigative approaches using destructive and non-destructive methodologies. *Geophys. Res. Abstr.,* 12:12259. (Abstract)

Kirschvink, J.L., 1980. The least-squares line and plane and the analysis of palaeomagnetic data. *Geophys. J. R. Astron. Soc.,* 62(3):699–718. **doi:10.1111/j.1365-246X.1980.tb02601.x**

Knight, R., and Nolen-Hoeksema, R., 1990. A laboratory study of the dependence of elastic wave velocities on pore scale fluid distribution. *Geophys. Res. Lett.,* 17(10):1529–1532. **doi:10.1029/GL017i010p01529**

Lever, M.A., Alperin, M., Engelen, B., Inagaki, F., Nakagawa, S., Steinsbu, B.O., Teske, A., and IODP Expedition Scientists, 2006. Trends in basalt and sediment core contamination during IODP Expedition 301. *Geomicrobiol. J.,* 23(7):517–530. **doi:10.1080/01490450600897245**

Lever, M.A., Heuer, V.B., Morono, Y., Masui, N., Schmidt, F., Alperin, M.J., Inagaki, F., Hinrichs, K.-U., and Teske, A., 2010. Acetogenesis in deep subseafloor sediments of the Juan de Fuca Ridge flank: a synthesis of geochemical, thermodynamic, and gene-based evidence. *Geomicrobiol. J.,* 27(2):183–211. **doi:10.1080/01490450903456681**

Lovell, M.A., Harvey, P.K., Brewer, T.S., Williams, C., Jackson, P.D., and Williamson, G., 1998. Application of FMS images in the Ocean Drilling Program: an overview. *In* Cramp, A., MacLeod, C.J., Lee, S.V., and Jones, E.J.W. (Eds.), *Geological Evolution of Ocean Basins: Results from the Ocean Drilling Program.* Geol. Soc. Spec. Publ., 131(1):287–303. **doi:10.1144/GSL.SP.1998.131.01.18**

Manheim, F.T., and Sayles, F.L., 1974. Composition and origin of interstitial waters of marine sediments, based on deep sea drill cores. *In* Goldberg, E.D. (Ed.), *The Sea* (Vol. 5): *Marine Chemistry: The Sedimentary Cycle:* New York (Wiley), 527–568.

Mazzullo, J.M., Meyer, A., and Kidd, R.B., 1988. New sediment classification scheme for the Ocean Drilling Program. *In* Mazzullo, J.M., and Graham, A.G. (Eds.),

Handbook for shipboard sedimentologists. ODP Tech. Note, 8:45–67. **doi:10.2973/odp.tn.8.1988**

Morono, Y., Terada, T., Masui, N., and Inagaki, F., 2009. Discriminative detection and enumeration of microbial life in marine subsurface sediments. *ISME J.,* 3(5):503–511. **doi:10.1038/ismej.2009.1**

Munsell Color Company, Inc., 2000. *Munsell Soil Color Chart*: New York (Gretag-Macbeth).

Murray, R.W., Miller, D.J., and Kryc, K.A., 2000. Analysis of major and trace elements in rocks, sediments, and interstitial waters by inductively coupled plasma–atomic emission spectrometry (ICP-AES). *ODP Tech. Note,* 29. **doi:10.2973/odp.tn.29.2000**

Nakagawa, S., Inagaki, F., Suzuki, Y., Steinsbu, B.O., Lever, M.A., Takai, K., Engelen, B., Sako, Y., Wheat, C.G., Horikoshi, K., and Integrated Ocean Drilling Program Expedition 301 Scientists, 2006. Microbial community in black rust exposed to hot ridge-flank crustal fluids. *Appl. Environ. Microbiol.,* 72(10):6789–6799. **doi:10.1128/AEM.01238-06**

Orcutt, B.N., Bach, W., Becker, K., Fisher, A.T., Hentscher, M., Toner, B.M., Wheat, C.G., and Edwards, K.J., 2011. Colonization of subsurface microbial observatories deployed in young ocean crust. *ISME J.* **doi:10.1038/ismej.2010.157**

Paillet, F.L., and Kim, K., 1987. Character and distribution of borehole breakouts and their relationship to in situ stresses in deep Columbia River basalts. *J. Geophys. Res., [Solid Earth],* 92(B7):6223–6234. **doi:10.1029/JB092iB07p06223**

Passchier, C.W., and Trouw, R.A.J., 1996. *Microtectonics:* Berlin (Springer-Verlag).

Ramsay, J.G., and Huber, M.I., 1987. *The Techniques of Modern Structural Geology* (Vol. 2): *Folds and Fractures:* New York (Acad. Press).

Rider, M.H., 1996. *The Geological Interpretation of Well Logs* (2nd ed.): Caithness (Whittles Publ.).

Schlumberger, 1989. *Log Interpretation Principles/Applications:* Houston (Schlumberger Educ. Serv.), SMP–7017.

Serra, O., 1984. *Fundamentals of Well-Log Interpretation* (Vol. 1): *The Acquisition of Logging Data:* Amsterdam (Elsevier).

Serra, O., 1986. *Fundamentals of Well-Log Interpretation* (Vol. 2): *The Interpretation of Logging Data*. Amsterdam (Elsevier).

Shepard, F.P., 1954. Nomenclature based on sand-silt-clay ratios. *J. Sediment. Res.,* 24(3):151–158.

Shipboard Scientific Party, 1989. Introduction and explanatory notes. *In* Robinson, P.T., Von Herzen, R., et al., P*roc. ODP, Init. Repts.,* 118: College Station, TX (Ocean Drilling Program), 3–23. **doi:10.2973/odp.proc.ir.118.101.1989**

Shipboard Scientific Party, 1991. Explanatory notes. *In* Taira, A., Hill, I., Firth, J.V., et al., *Proc. ODP, Init. Repts.,* 131: College Station, TX (Ocean Drilling Program), 25–60. **doi:10.2973/odp.proc.ir.131.104.1991**

Shipboard Scientific Party, 1992a. Explanatory notes. *In* Behrmann, J.H., Lewis, S.D., Musgrave, R.J., et al., *Proc. ODP, Init. Repts.,* 141: College Station, TX (Ocean Drilling Program), 37–71. **doi:10.2973/odp.proc.ir.141.105.1992**

Shipboard Scientific Party, 1992b. Explanatory notes. *In* Davis, E.E., Mottl, M.J., Fisher, A.T., et al., *Proc. ODP, Init. Repts.,* 139: College Station, TX (Ocean Drilling Program), 55–97. **doi:10.2973/odp.proc.ir.139.104.1992**

Shipboard Scientific Party, 1992c. Explanatory notes. *In* Dick, H.J.B., Erzinger, J., Stokking, L.B., et al., *Proc. ODP, Init. Repts.,* 140: College Station, TX (Ocean Drilling Program), 5–33. **doi:10.2973/odp.proc.ir.140.101.1992**

Shipboard Scientific Party, 1992d. Explanatory notes. *In* Parson, L., Hawkins, J., Allan, J., et al., *Proc. ODP, Init. Repts.,* 135: College Station, TX (Ocean Drilling Program), 49–79. **doi:10.2973/odp.proc.ir.135.102.1992**

Shipboard Scientific Party, 1993a. Explanatory notes. *In* Alt, J.C., Kinoshita, H., Stokking, L.B., et al., *Proc. ODP, Init. Repts.,* 148: College Station, TX (Ocean Drilling Program), 5–24. **doi:10.2973/odp.proc.ir.148.101.1993**

Shipboard Scientific Party, 1993b. Explanatory notes. *In* Gillis, K., Mével, C, Allan, J., et al., *Proc. ODP, Init. Repts.,* 147: College Station, TX (Ocean Drilling Program), 15–42. **doi:10.2973/odp.proc.ir.147.102.1993**

Shipboard Scientific Party, 1995. Explanatory notes. *In* Cannat, M., Karson, J.A., Miller, D.J., et al., *Proc. ODP, Init. Repts.,* 153: College Station, TX (Ocean Drilling Program), 15–42. **doi:10.2973/odp.proc.ir.153.10X.1995**

Shipboard Scientific Party, 1999. Explanatory notes. *In* Barker, P.F., Camerlenghi, A., Acton, G.D., et al., *Proc. ODP, Init. Repts.,* 178: College Station, TX (Ocean Drilling Program), 1–66. **doi:10.2973/odp.proc.ir.178.104.1999**

Shipboard Scientific Party, 2003. An in situ section of upper oceanic crust formed by superfast seafloor spreading. *ODP Prelim. Rept.,* 206: College Station, TX (Ocean Drilling Program). **doi:10.2973/odp.pr.206.2003**

Shipboard Scientific Party, 2004. Explanatory notes. *In* Tucholke, B.E., Sibuet, J.-C., Klaus, A., et al., *Proc. ODP, Init. Repts.,* 210: College Station, TX (Ocean Drilling Program), 1–69. **doi:10.2973/odp.proc.ir.210.102.2004**

Smith, D.C., Spivack, A.J., Fisk, M.R., Haveman, S.A., and Staudigel, H., 2000a. Tracer-based estimates of drilling-induced microbial contamination of deep sea crust. *Geomicrobiol. J.,* 17(3):207–219. **doi:10.1080/01490450050121170**

Smith, D.C., Spivack, A.J., Fisk, M.R., Haveman, S.A., Staudigel, H., and the Leg 185 Shipboard Scientific Party, 2000b. Methods for quantifying potential microbial contamination during deep ocean coring. *ODP Tech. Note, 2*8. **doi:10.2973/odp.tn.28.2000**

Twiss, R.J., and Moores, E.M., 1992. *Structural Geology:* New York (Freeman).

Vacquier, V., 1985. The measurement of thermal conductivity of solids with a transient linear heat source on the plane surface of a poorly conducting body. *Earth Planet. Sci. Lett.,* 74(2–3):275–279. **doi:10.1016/0012-821X(85)90027-5**

Von Herzen, R., and Maxwell, A.E., 1959. The measurement of thermal conductivity of deep-sea sediments by a needle-probe method. *J. Geophys. Res.,* 64(10):1557–1563. **doi:10.1029/JZ064i010p01557**

Wentworth, C.K., 1922. A scale of grade and class terms for clastic sediments. *J. Geol.,* 30(5):377–392. **doi:10.1086/622910**

Wheat, C.G., Jannasch, H.W., Fisher, A.T., Becker, K., Sharkey, J., and Hulme, S., 2010. Subseafloor seawater-basalt-microbe reactions: continuous sampling of borehole fluids in a ridge flank environment. *Geochem., Geophys., Geosyst.,* 11(7):Q07011. **doi:10.1029/2010GC003057**

Publication: 5 September 2011
MS 327-102

Figure F1. Integrated Ocean Drilling Program (IODP) naming convention for Expedition 327 sites, holes, cores, and samples.

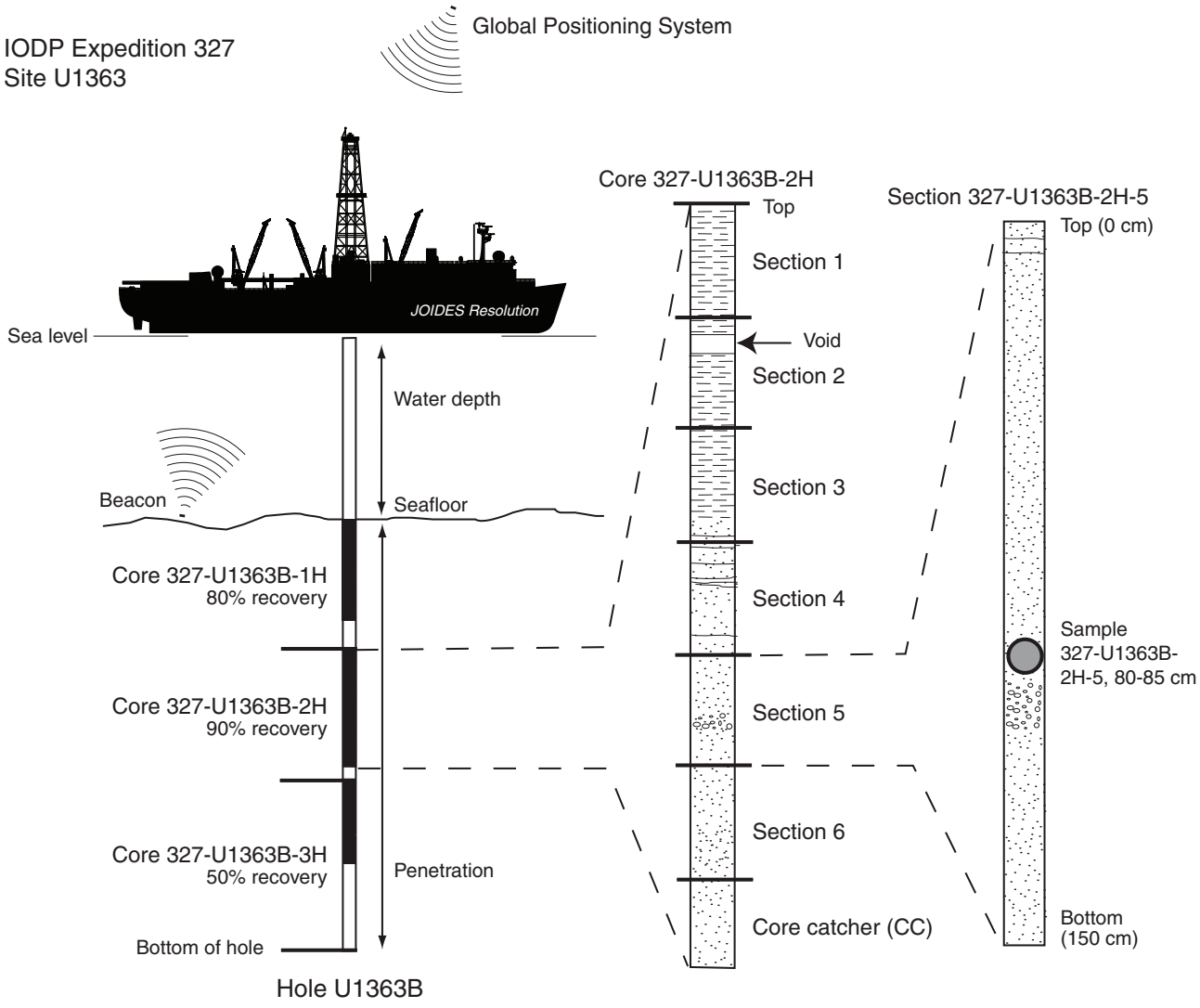

Figure F2. Hard rock visual core description legend, Expedition 327. ICP-AES = inductively coupled plasma–atomic emission spectroscopy.

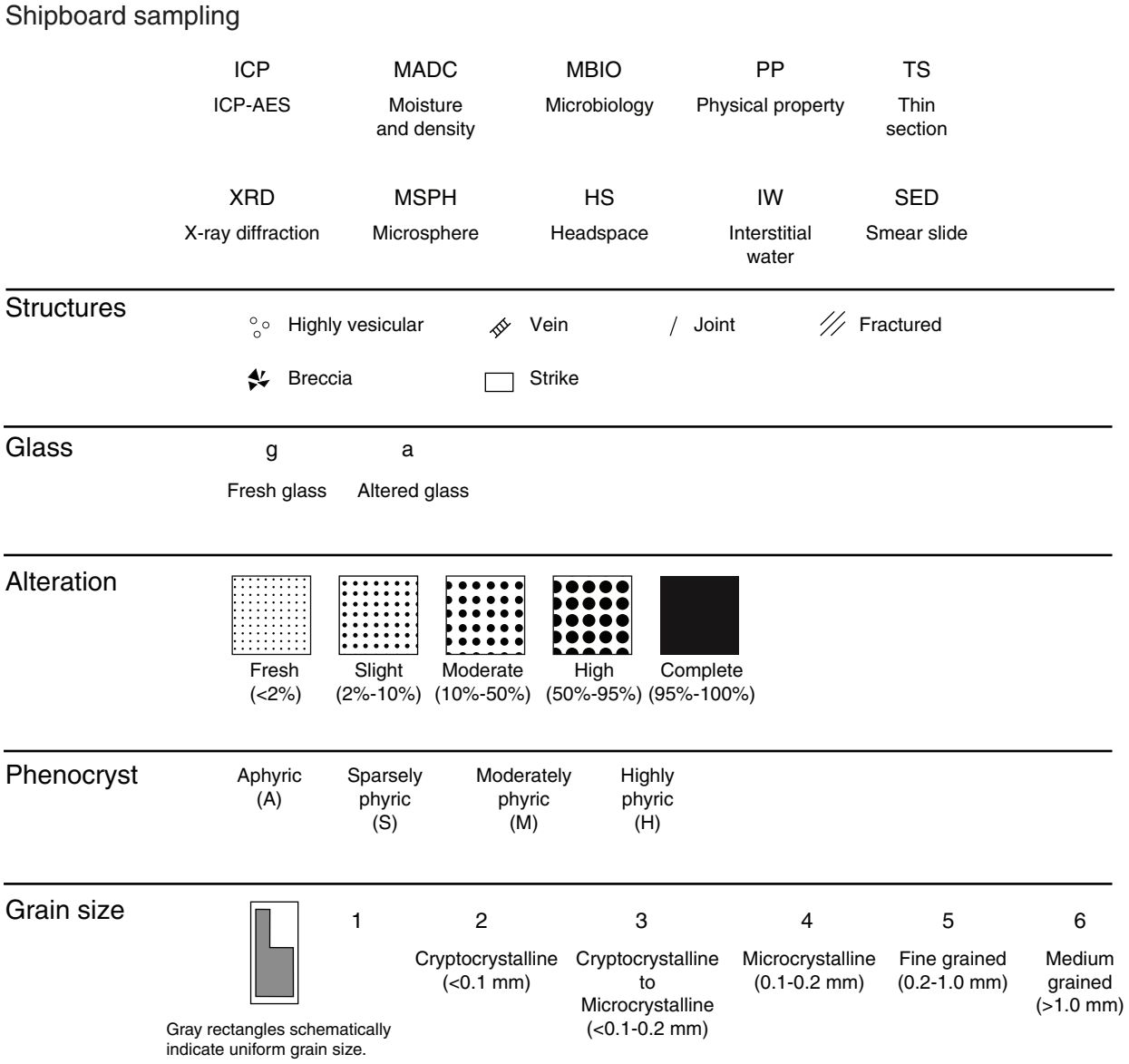

Figure F3. Example of thin section table, Expedition 327.

THIN SECTION:	327-U1362A-3R-2-W, 79-81 cm		Piece No:		Unit: 1A	OBSERVER: JR, THIN SECTION 9	
ROCK NAME:	basalt						
WHERE SAMPLED:	pillow interior (multilayer alteration halo)						
GRAINSIZE:	cryptocrystalline						
TEXTURE:	subophitic, vesicular, intersertal						
PRIMARY MINERALOGY	PERCENT PRESENT	PERCENT ORIGINAL	SIZE(mm) min.	max.	mode	MORPHOLOGY	COMMENTS
PHENOCRYSTS							
pyroxene	2	2.2	0.2	1.28	0.3		
plagioclase	4.8	5	0.4	1.52	1	euhedral	Occurs singly and as mono- and polymineralic glomeroporphyritic clots with pyroxene
olivine	trace	1	0.7	0.8		anhedral	Rounded. Entirely pseudomorphed by celadonite and saponite
MICROPHENOCRYST							
GROUNDMASS							
plagioclase	12	20	<0.1	1.2	0.4	acicular	Pseudomorphed by saponite and celadonite
pyroxene	10	18	<0.1	0.2	0.1	anhedral	Pseudomorphed by saponite and celadonite
mesostasis	6	52					Almost entirely replaced by saponite
SECONDARY MINERALOGY							
saponite	49						Saponite filling vesicles, replacing groundmass, phenocrysts and mesostasis
iron oxides	2						Feox filling vesicles associated with alteration halo
oxides	1						Oxides replacing mesostasis
celadonite	9						Celadonite filling vesicles, replacing mesostasis and olivine, all associated with alteration halo
VESICLES MINERALOGY	PERCENT MODAL ABUNDANCE	PERCENT FILLED	SIZE(mm) min.	max.	mode	SHAPE	COMMENTS
cladonite, saponite, iron oxides	5.2	35	<0.1	0.6	0.5	moderately spherical	Vesicle fill (alteration halo): celadonite lining with feox core, celadonite, saponite lining with feox core, layered mixed saponite + celadonite, celadonite, saponite, celadonite, feox. Vesicle fill (background alteration): saponite lining, empty.
VEINS		FILLING	THICKNESS(mm)			SHAPE	COMMENTS
N/A							
SUMMARY DESCRIPTION	Multilayered green and dark grey halo contains feox and celadonite which fill vesicles and replace mesostasis.						

Figure F4. Sketch of vein morphologies, Expedition 327.

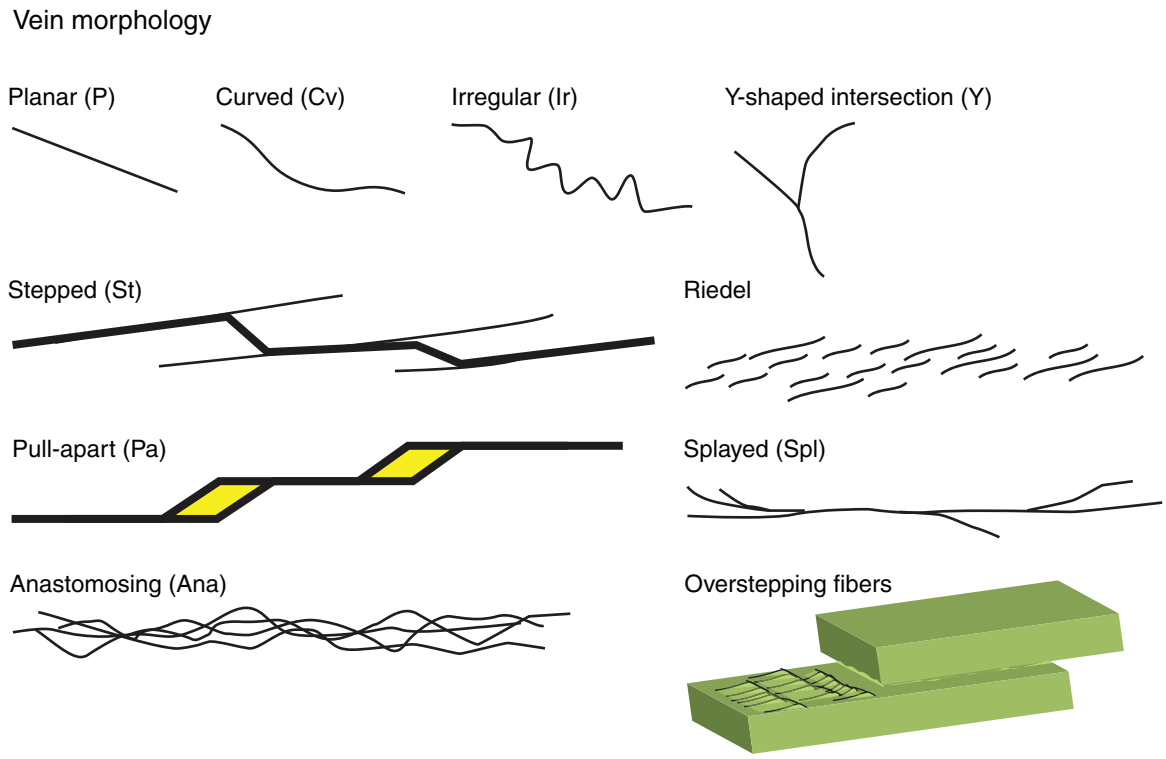

Figure F5. Sketch of archive half showing conventions used during Expedition 327 for measuring the orientation of structural features. IODP = Integrated Ocean Drilling Program.

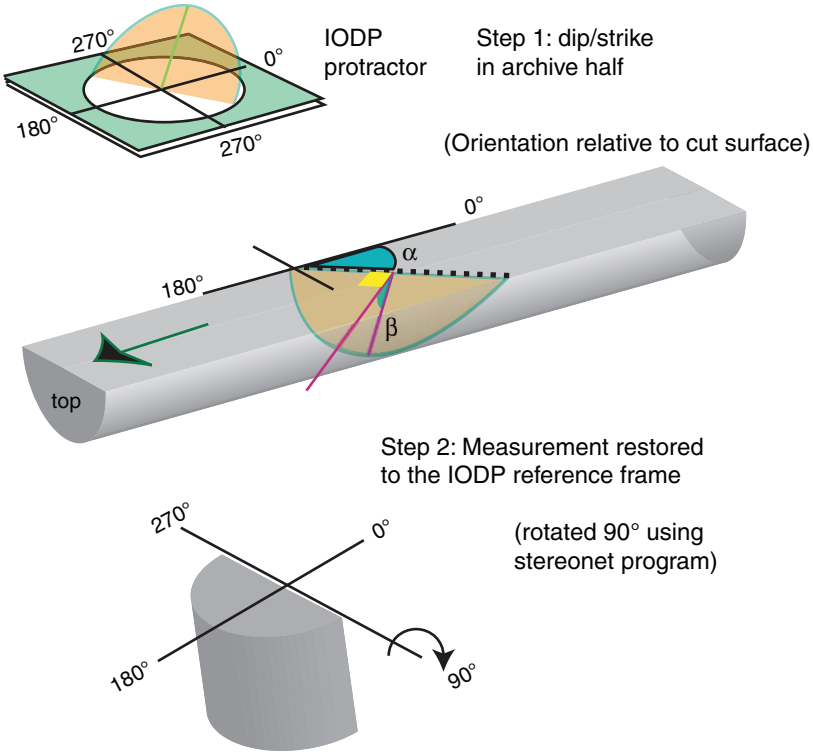

Figure F6. Ternary plots of lithology naming scheme used during Expedition 327. Modified from Shipboard Scientific Party (2004). Lower ternary plot follows Shepard (1954).

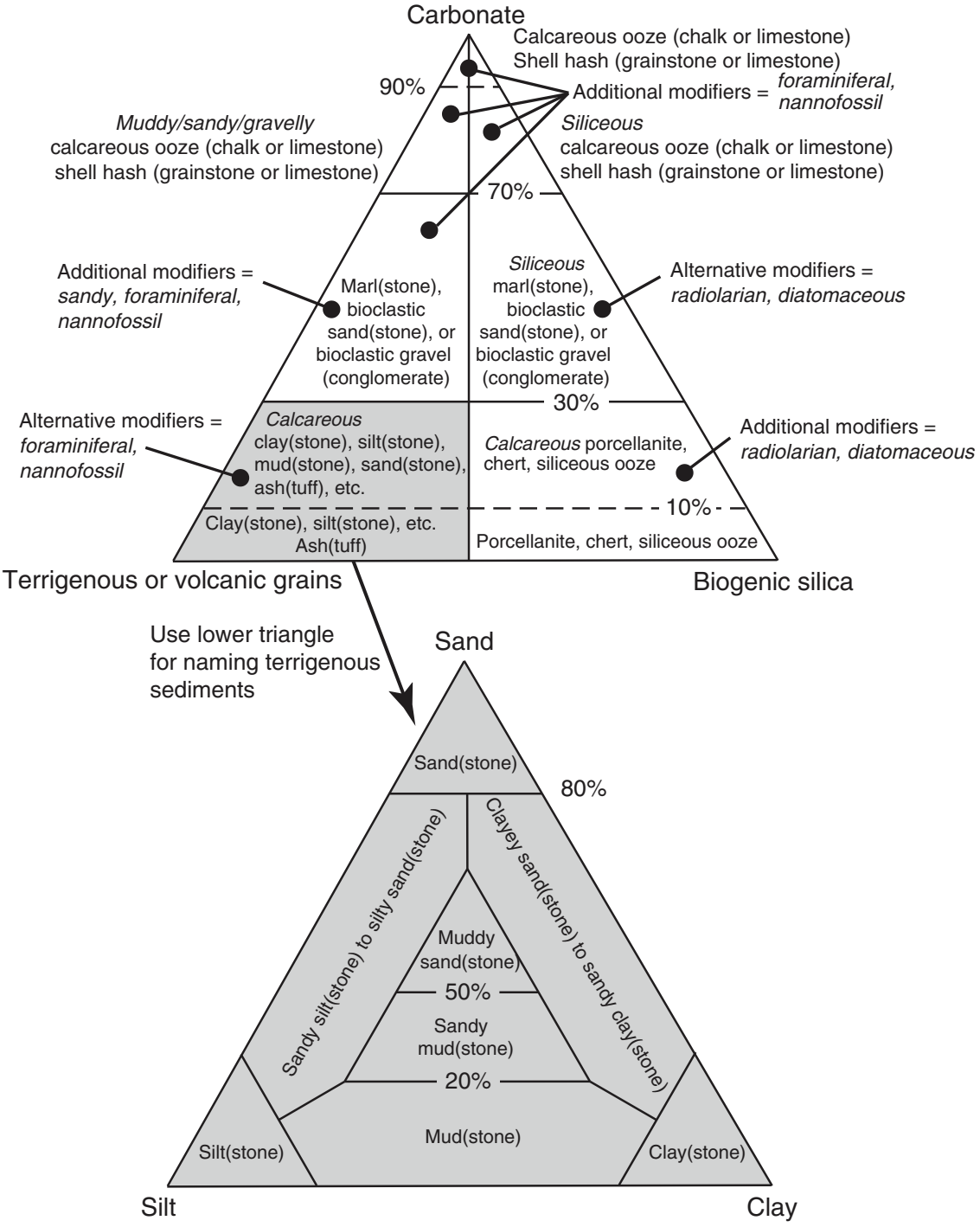

Figure F7. Legend for Expedition 327 sediment visual core descriptions ("barrel sheets"), including drilling disturbance, lithology, sedimentary and tectonic structures, and sample types. ICP-AES = inductively coupled plasma–atomic emission spectroscopy.

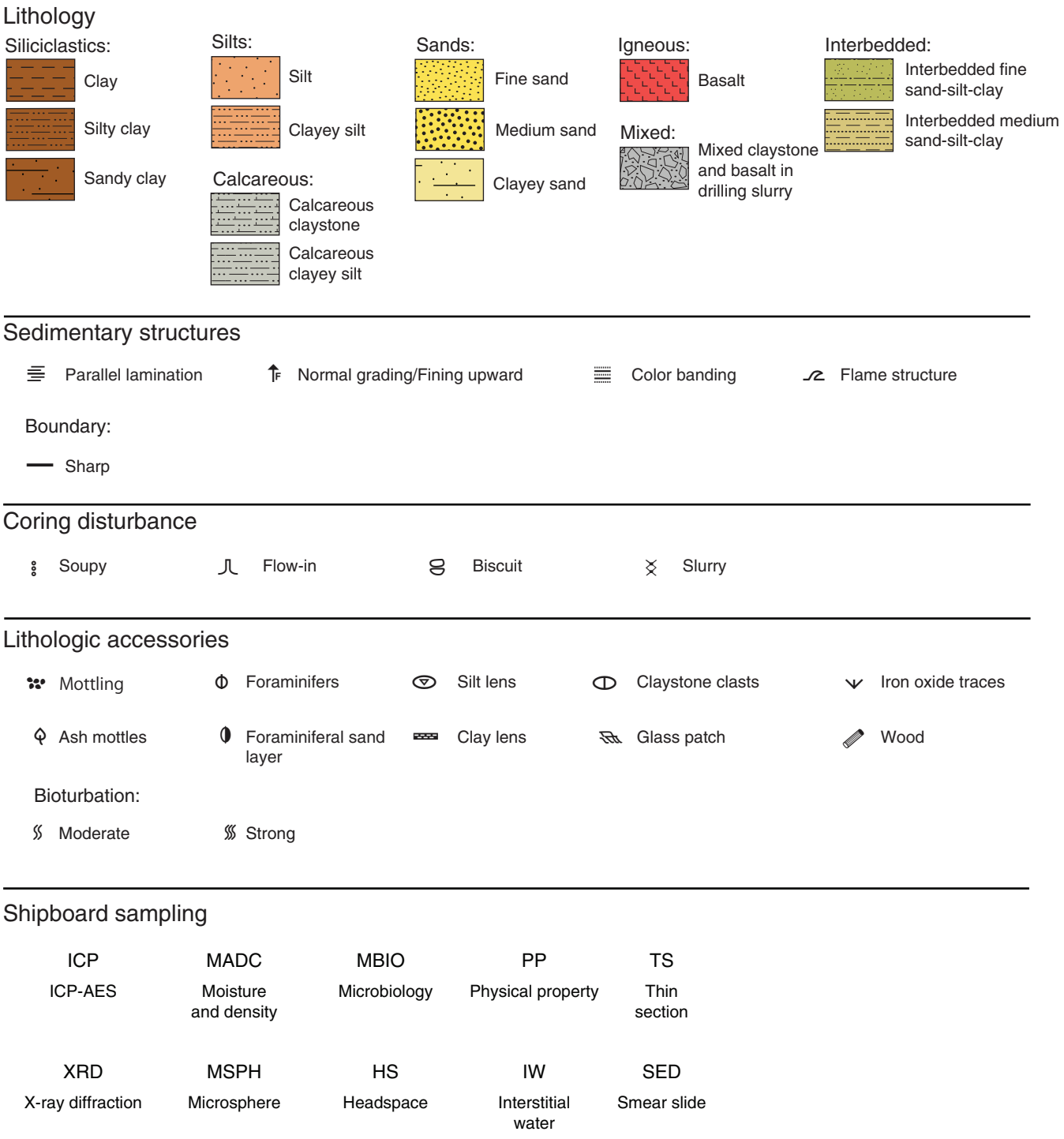

Figure F8. Photograph of custom stainless steel box with hinged lid and metal plate for hard rock microbiology processing, donated to the *JOIDES Resolution* by Dr. Katrina Edwards (University of Southern California). Before a hard rock sample was processed for microbiology, the inside of the box was sprayed with ethanol and flame sterilized. The inner metal plate helps provide support when breaking rocks open with a hammer and chisel (also flame sterilized).

Figure F9. Correlation of recorded and reference waveforms used to obtain traveltime. **A.** Recorded waveform without sample. **B.** Enlarged first arrival of the waveform in A. **C.** Recorded waveform with sample. **D.** Enlarged first arrival of the waveform in C. **E.** Overlapped waveforms considering the traveltime within the sample (ΔT). **F.** Enlarged first arrival of the waveform in E.

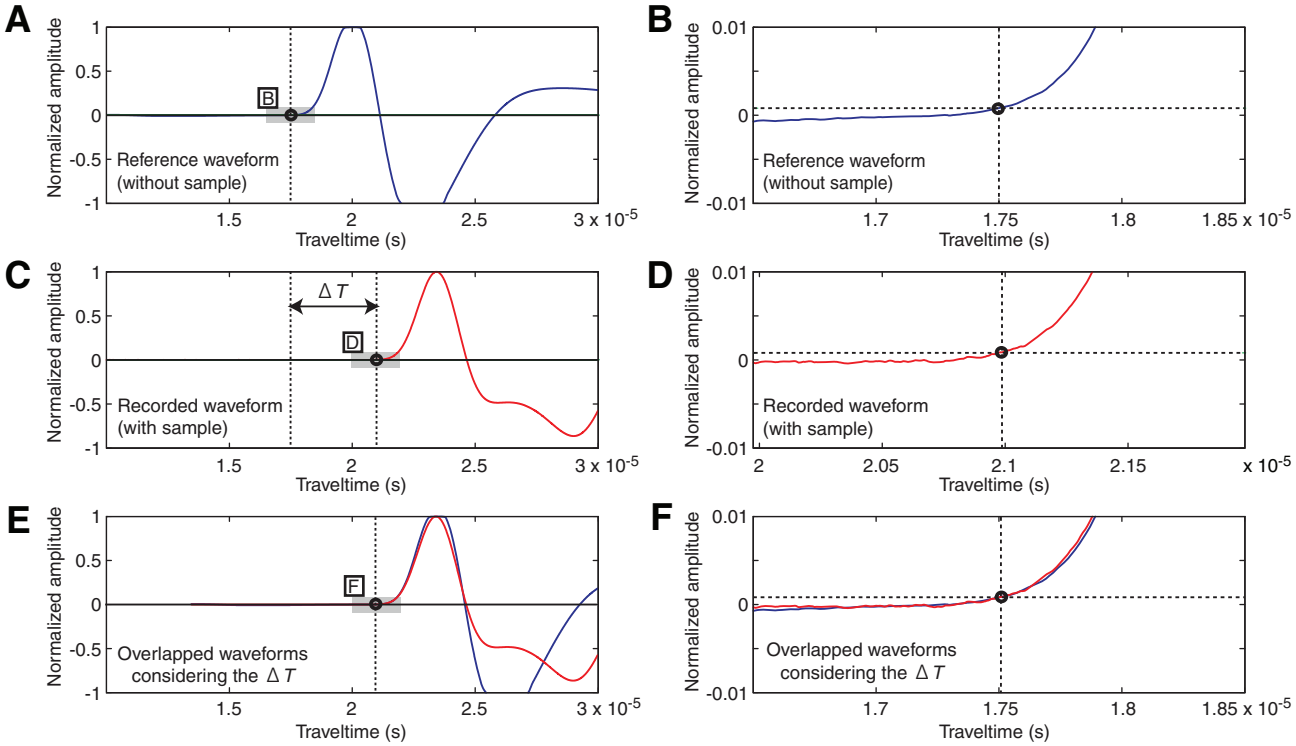

Figure F10. Diagram of the magnetic coordinate system for working- and archive-half core sections used during Expedition 327.

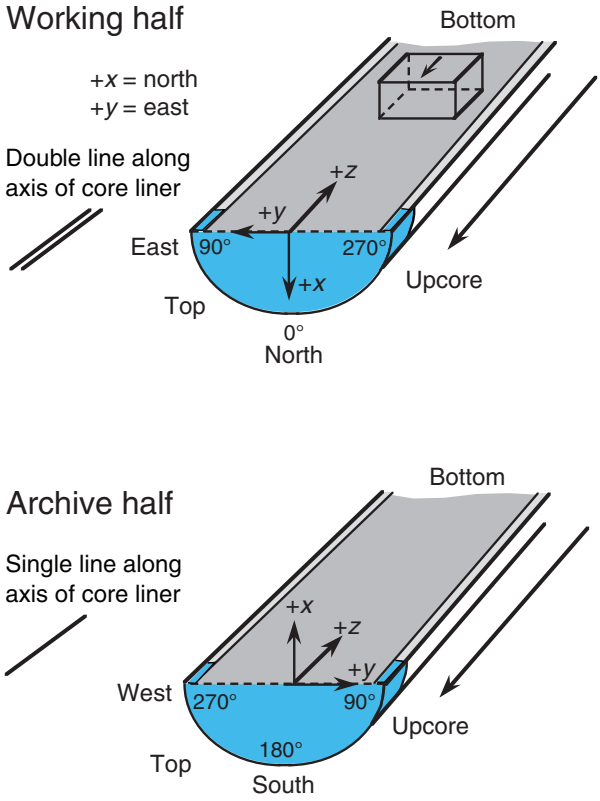

Figure F11. Geomagnetic polarity timescale used for Expedition 327, based on Cande and Kent (1995). Black = normal polarity, white = reversed polarity. Absolute ages, geologic periods, and magnetic chron terminology are also provided.

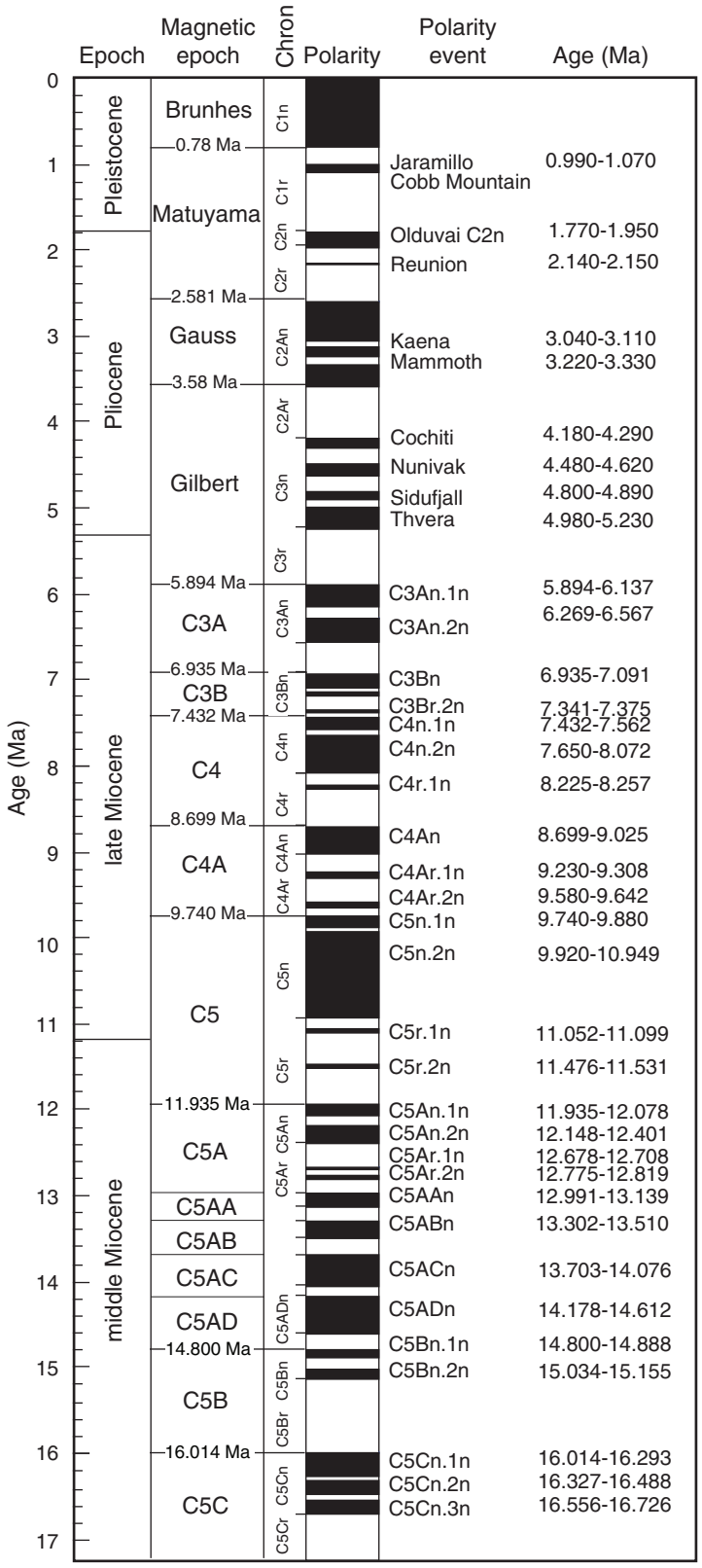

Figure F12. Schematic of Hole U1362A wireline logging tool string configuration. Lengths are in meters.

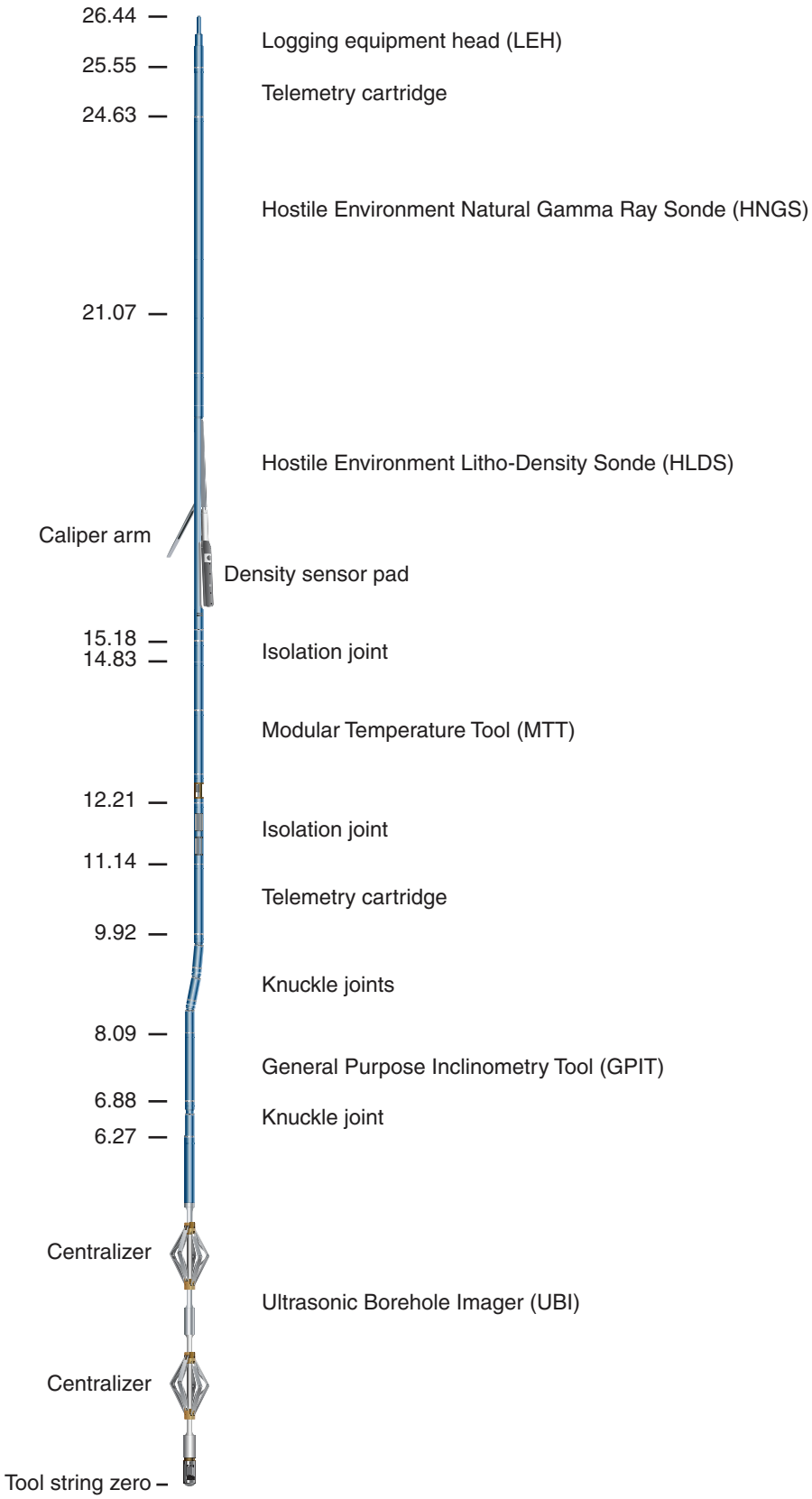

Table T1. IODP depth scale terminology, Expedition 327. (See table notes.)

Depth scale	Acronym	Origin	Method description	Submethod	Unit	Previous name*	Previous unit*
Drillers depth scale:							
Drilling depth below rig floor	DRF	Drill floor	Add lengths of all drill string components deployed beneath rig floor from bit to point on rig floor where length of deployed portion of last string is measured	Describe how drill string component length and length deployed at rig floor are measured	m	Depth	mbrf
Drilling depth below seafloor	DSF	Seafloor	Subtract distance between rig floor and sea level from an estimate of seafloor depth at DRF scale using one of the submethods	Specify submethod used: A. Tag seafloor B. Mudline core C. Visual control D. Inherit depth E. Other	m	Depth	mbsf
Core depth scale:							
Core depth below seafloor	CSF	Seafloor	Measure core sample or measurement offset below core top and add to core top DSF scale using one of the submethods	Specify submethod used: A. Let overlap if long B. Scale if long C. Other	m	Depth	mbsf
Core composite depth below seafloor	CCSF	Seafloor	Align cores from one hole or multiple adjacent holes using one of the submethods to create a newly constructed depth scale	Specify submethod used: A. Append if long B. Scale by factor C. Correlate features D. Splice E. Other	m	Depth	mcd
Wireline depth scale:							
Wireline log depth below rig floor	WRF	Drill floor	Measure length of wireline extended beneath rig floor	Describe how wireline length deployed at rig floor is measured	m	Depth	mbrf
Wireline log depth below seafloor	WSF	Seafloor	Subtract distance between rig floor and sea level from an estimate of seafloor depth at WRF scale using one of the submethods	Specify submethod used: A. Seafloor signal B. Drilling depth C. Inherit depth D. Other	m	Depth	mbsf
Wireline log speed-corrected depth below seafloor	WSSF	Seafloor	Correct for irregular motion of tool during logging using accelerometer data; use for high-resolution logs such as FMS	Describe measurement method if applicable	m	Depth	mbsf
Wireline log matched depth below seafloor	WMSF	Seafloor	Pick log data from one run as reference and map other run data using several tie points	Describe reference log and number/type of tie points used	m	Depth	mbsf

Notes: * = ODP depth scale conventions. Drillers depth scale is based on length of drill pipe lowered below drill floor. Core depth scale is based on actual length of core recovered and drillers depth and can vary with time as core expands or contracts. Thus, core depth is technically not a depth but can be used to derive a depth by cumulating all core lengths. Wireline depth scale is based on wireline length between downhole tool and shipboard winch. FMS = Formation MicroScanner. See IODP Depth Scales Terminology at www.iodp.org/program-policies/.

Table T2. Analytical conditions for hard rock ICP-AES runs, Expedition 327.

Element	Wavelength (nm)	Integration time (s)	Power (kW)
Al	308.215, 396.152	30	1.2
Ba	493.409	30	1.2
Ca	317.933	30	1.2
Co	228.615	30	1.2
Cr	283.563	30	1.2
Cu	324.754	30	1.2
Fe	238.204, 239.563	30	1.2
K	769.897	30	1.2
Mg	280.271, 285.213	30	1.2
Mn	257.610, 259.372	30	1.2
Na	588.995, 589.592	30	1.2
Ni	231.604	30	1.2
P	214.914	30	1.2
Sc	361.383	30	1.2
Si	250.690, 251.611	30	1.2
Sr	407.771, 421.552	30	1.2
Ti	337.280	30	1.2
V	292.401	30	1.2
Zn	213.856	30	1.2
Zr	339.198, 343.823	30	1.2

Table T3. ICP-AES replicate analyses of BCR-2 standards, reported as intensity, Expedition 327.

Element	Wavelength (nm)	1	1	1	2	2	2	3	3	3	Average (N = 9)	Standard deviation	Precision (%)
Si	250.690	3375383	3399437	3423138	3358339	3348577	3348684	3286866	3300356	3326570	3351928	43984	1.31
Si	251.611	14641060	14450862	14660201	14376502	14303297	14413689	14058824	14161049	14251442	14368547	201605	1.40
Al	308.215	7397639	7429428	7418285	7335153	7335067	7347768	7228511	7197781	7289314	7330994	80662	1.10
Al	396.152	29400547	29397408	29435365	28991668	28948284	28978773	28602873	28496541	28709420	28995653	354710	1.22
Fe	238.204	3083933	3114678	3215009	3045975	3038504	3050897	2985697	2985002	3024592	3060476	71352	2.33
Fe	239.563	5754496	5769832	5802294	5618850	5657333	5638643	5554112	5540544	5576758	5656985	97292	1.72
Mn	257.610	736192	734699	735656	723313	721843	725207	701355	700464	709073	720866	14172	1.97
Mn	259.372	578663	577827	579783	569542	572697	573323	559769	557172	561654	570047	8583	1.51
Mg	280.271	37235195	37227075	37528154	36710038	36760012	36894503	36280117	36239557	36437531	36812465	452076	1.23
Mg	285.213	4599102	4603572	4620929	4465264	4468367	4487431	4359473	4357697	4406444	4485364	102689	2.29
Ca	317.933	15820573	15803974	15869425	15541642	15460573	15571987	15287183	15236845	15418218	15556713	232485	1.49
Na	588.995	59434666	59227129	59418322	59028740	58603432	58755508	58311336	57534862	58119473	58714830	642038	1.09
Na	589.592	22500161	22544060	22573293	22083279	22023006	22169024	21701809	21706435	21841493	22126951	347497	1.57
K	769.897	10034241	10063136	10110639	9942338	9951966	9943848	9741260	9724447	9825577	9926384	137254	1.38
Ti	337.280	4904566	4906985	4943865	4808742	4789677	4810526	4686079	4689546	4726791	4807420	95795	1.99
P	214.914	16198	15794	16541	15481	15746	15728	15807	15324	16008	15847	365	2.30
Ba	493.409	3356450	3329556	3383497	3297277	3335664	3314260	3248021	3297853	3285440	3316446	40309	1.22
Co	228.615	17034	17166	17104	16900	16744	15792	15990	15969	15994	16521	571	3.46
Cr	283.563	52980	52102	53240	52669	51464	54001	51153	50555	53137	52366	1126	2.15
Cu	324.754	32909	31564	32837	35051	35393	31658	36271	31684	33877	33471	1769	5.28
Ni	231.604	3924	4513	3421	4477	4521	4216	4543	3960	3772	4149	403	9.70
Sc	361.383	248648	249693	246403	247593	250334	245707	242759	241833	242738	246189	3170	1.29
Sr	407.771	8289997	8298651	8343877	8279278	8312437	8291903	8222769	8247891	8287833	8286071	34926	0.42
V	292.401	222691	223428	225983	221724	222186	222802	217866	219102	219719	221722	2478	1.12
Zn	213.856	33087	32532	32843	32757	32227	32541	32419	32247	32102	32528	322	0.99
Zr	339.198	274722	271635	281467	273333	273457	275655	271876	271279	267806	273470	3760	1.37
Zr	343.823	311016	309698	314301	297770	306221	300503	299263	302388	307398	305395	5732	1.88

Table T4. Wireline tool string downhole measurements, Expedition 327. (See table notes.)

Tool	Measurement	Sampling interval (cm)	Approximate vertical resolution (cm)
LEH	Spontaneous potential (qualitative)	15	NA
HNGS	Spectral gamma ray	15	51
HLDS	Bulk density, PEF, caliper	15	38
MTT	Borehole fluid temperature	15	NA
GPIT	Tool orientation, downhole motion	15	NA
UBI	Ultrasonic image, caliper	0.5–2.5	0.5–2.5

Notes: LEH, HNGS, HLDS, GPIT, and UBI are trademarks of Schlumberger. For definitions of tool acronyms, see Table T5. NA = not applicable. PEF = photoelectric effect.

Table T5. Acronyms and units used for downhole wireline tools and measurements, Expedition 327. (See table notes.)

Tool	Output	Description	Unit
LEH		Logging equipment head	
	SP	Spontaneous potential (qualitative)	mV
	DF	Cable head tension	lbf
	TENS	Surface cable tension	lbf
	CS	Surface cable speed	m/h
HNGS		Hostile Environment Natural Gamma Ray Sonde	
	HSGR	Standard (total) gamma ray	API
	HCGR	Computed gamma ray (HSGR minus uranium contribution)	API
	HFK	Potassium (K)	wt%
	HTHO	Thorium (Th)	ppm
	HURA	Uranium (U)	ppm
	HBHK	Borehole potassium	wt%
HLDS		Hostile Environment Litho-Density Sonde	
	RHOM	Corrected bulk density	g/cm^3
	PEFL	Photoelectric effect	b/e^-
	LCAL	Long-axis borehole caliper	inch
	DRH	Bulk density correction	g/cm^3
	NRHB	Bulk density	g/cm^3
MTT		Modular Temperature Tool	
	WTEP	Borehole fluid temperature	°C
GPIT		General Purpose Inclinometry Tool	
	DEVI	Hole deviation	degrees
	HAZI	Hole azimuth	degrees
	F*x*, F*y*, F*z*	Earth's magnetic field (three orthogonal components)	Oe
	A*x*, A*y*, A*z*	Acceleration (three orthogonal components)	m/s^2
	FNOR	Magnetic field total movement	Oe
	FINC	Magnetic field inclination	degrees
	RB	Pad 1 relative bearing	degrees
	P1AZ	Pad 1 azimuth	degrees
UBI		Ultrasonic Borehole Imager	
	FTED	Median borehole radius	inch
	FT25	Lower quartile borehole radius	inch
	FT75	Upper quartile borehole radius	inch
	AMED	Median amplitude	db
	AM25	Lower quartile amplitude	db
	AM75	Upper quartile amplitude	db
	TTVIEW	Transit time image	µs
	AWVIEW	Amplitude window image	db

Notes: LEH, HNGS, HLDS, GPIT, and UBI are trademarks of Schlumberger. For the complete list of acronyms used in IODP and for additional information about tool physics, consult IODP-USIO Science Services, LDEO, at iodp.ldeo.columbia.edu/TOOLS_LABS/tools.html.